Nuclear Science and Engineering

ISSN: (Print) (Online) Journal homepage: https://www.tandfonline.com/loi/unse20

Demonstrating Computational Equivalence Between Continuous and Discrete Adjoint Methods by Calculating Time-Dependent Adjoint Solutions with Neutron Diffusion Models

Zeyun Wu, Cihang Lu & Tao Liu

To cite this article: Zeyun Wu, Cihang Lu & Tao Liu (2023) Demonstrating Computational Equivalence Between Continuous and Discrete Adjoint Methods by Calculating Time-Dependent Adjoint Solutions with Neutron Diffusion Models, Nuclear Science and Engineering, 197:6, 1213-1238, DOI: 10.1080/00295639.2022.2143207

To link to this article: https://doi.org/10.1080/00295639.2022.2143207

Published online: 01 Feb 2023.

NUCLEAR SCIENCE AND ENGINEERING · VOLUME 197 · 1213–1238 · JUNE 2023

DOI: https://doi.org/10.1080/00295639.2022.2143207

Demonstrating Computational Equivalence Between Continuous and Discrete Adjoint Methods by Calculating Time-Dependent Adjoint Solutions with Neutron Diffusion Models

Zeyun Wu,* Cihang Lu,† and Tao Liu

Virginia Commonwealth University, Department of Mechanical and Nuclear Engineering, 401 West Main Street, Richmond, Virginia 23284-3015

Received April 17, 2022
Accepted for Publication October 31, 2022

Abstract — *The continuous adjoint method and the discrete adjoint method are two alternative approaches used to calculate adjoint solutions for adjoint systems. The continuous adjoint method derives adjoint equations analytically from continuous forward equations and then solves the adjoint equations either analytically or numerically in a discretized form whereas the discrete adjoint method calculates the adjoint solutions directly from the discretized forward equations. With regard to the methodology development and calculation procedure, distinct differences are well recognized between the two methods. For certain reasons, both methods are exclusively preferred and commonly used by different computational communities, but limited studies clarify the connections between the two adjoint methods from either of the communities.*

This paper demonstrates the computational equivalence between the continuous and discrete adjoint methods by investigating time-dependent adjoint solutions to the two-group neutron diffusion model in nuclear reactor analysis problems using both methods. Adjoint solutions can be used to estimate system parameters for reactor safety analysis. Appropriate final state conditions for the adjoint systems are specified in both of the methods, and the conditions are clarified with proper physical explanations. With the help of an event-based case study on neutron diffusion models, the accuracy of the time-dependent adjoint fluxes obtained from both methods is verified, and the pros and cons of both adjoint methods are examined. More importantly, the computational equivalence of both methods is demonstrated when they are applied to multigroup neutron diffusion systems. The advantage of calculating time-dependent adjoint fluxes by directly solving time-dependent adjoint systems rather than taking steady-state approximations as in common practice is also demonstrated.

Keywords — *Time-dependent adjoint flux, two-group diffusion model, continuous adjoint method, discrete adjoint method.*

Note — *Some figures may be in color only in the electronic version.*

I. INTRODUCTION

The adjoint flux, which can be understood as the importance of particles, is the adjoint solution to the neutron transport/diffusion equations. The adjoint flux can be employed in nuclear engineering for reactor design optimization. More importantly, the adjoint flux is indispensable for adjoint sensitivity analysis of some system parameters that are crucial for reactor safety. The adjoint flux can be used to estimate both perturbations in reactivity, via the Rayleigh quotient (derived from the perturbation theory),[1] and kinetics parameters by utilizing the point-reactor kinetics theory.[2] Compared to the forward sensitivity method, the adjoint sensitivity method is

*E-mail: zwu@vcu.edu
†Currrent address: Nuclear Science & Technology Department, Brookhaven National Laboratory; clu@bnl.gov

more cost-effective in cases where there are a large number of sensitivity parameters and relatively fewer objective functions.[3,4] The latter case is encountered more often in nuclear engineering as most reactor analysis problems have very few objective functions. For example, in a criticality problem, the sensitivity parameters under investigation include core geometries, material properties, temperatures of various components of the core, etc., while the only objective function of interest is reactivity.[5,6]

The adjoint method for sensitivity analysis was first employed in the nuclear industry in the 1940s to estimate the eigenvalues of transport equations.[7] The physical basis of using adjoint solutions in transport and diffusion problems is provided in Ref. 8. The adjoint method was later widely used in different research fields, including meteorology,[9,10] electricity generation,[11] and aerodynamics.[12,13] In nuclear engineering, since the early 1980s, Cacuci et al.[14] and Cacuci[15,16] performed extensive studies using the adjoint sensitivity method. The applications included steady-state reactor analysis problems,[17] steady-state and transient single-fluid-flow problems[18] and two-fluid-flow problems,[19–21] etc. The adjoint sensitivity can be investigated with two distinct methods, namely, the continuous adjoint method[17] and the discrete adjoint method.[22,23] When the continuous method is used, the adjoint equations are derived analytically from the forward equations and then solved either analytically or numerically in a discretized form. When the discrete method is employed, the adjoint equations are calculated directly from the discretized forward equations. In both methods, the adjoint solutions are indispensable and need to be calculated to form the sensitivity information.

Because of differences that exist in the discrete and continuous forms of adjoint systems, the approaches employed to calculate adjoint solutions bear some apparent differences. For certain historical reasons, it is interesting to notice that both of these methods are exclusively preferred and commonly used by different computational communities. For example, the continuous adjoint method is well recognized and widely used in the nuclear engineering community for perturbation and general perturbation applications[1,5,24] while the discrete adjoint method is commonly adopted in the aerospace engineering community for sensitivity analysis.[25,26] However, limited studies investigate the connections between the two methods. This also indicates limited conversations between different scientific communities with regard to similar applications. Moreover, multigroup neutron diffusion systems differ from other systems in that numerous variables, including the neutron flux in different energy groups and the delayed neutron precursor (DNP) concentrations of different families, of reactor analysis problems are tightly coupled. Although continuous and discrete adjoint methods recently have been compared in some applications such as thermal-hydraulic problems,[7,27] very few discussions comparing both methods as they apply to nuclear reactor analysis using multigroup diffusion models exist in the literature.

Partly because of excessive computational cost, adjoint fluxes are calculated usually only at steady states in reactor calculations, and further, these adjoint fluxes are used to estimate parameters at time-dependent conditions.[2,28,29] Although many of the results from steady-state systems can be readily extended to time-dependent systems,[4] several unique features can be obtained only from the time-dependent system. An example is the importance of particles at a certain moment in time to a specific response at another moment. In addition to boundary conditions, initial conditions are needed for computation of the time-dependent forward system. On the contrary, final conditions are needed for computation of time-dependent adjoint systems that are solved backward in time.[22,27,30] Discussions on time-dependent adjoint fluxes and final condition specifications are also very limited in the literature.

Motivated by these observations, we carried out the study in this paper aiming at two major objectives. The first objective is to provide insights into time-dependent adjoint fluxes and to discuss appropriate final conditions for time-dependent adjoint systems. The second objective is to investigate and understand the differences that exist in the methodologies and implementation procedures between the continuous and the discrete adjoint methods in search of time-dependent adjoint fluxes for reactor analysis problems. Computational equivalence in the calculations of both methods is sought through comparative study. This study employs an event-based case modeled by two-group neutron diffusion models to demonstrate the application of both adjoint calculation methods for time-dependent reactor analysis problems.

The rest of the paper is organized as follows. Section II introduces the event used as the case study in this work, followed by the steady-state and forward transient calculations of the case study. These calculations are performed and verified by existing references. Section III presents the continuous adjoint method and the calculation of the time-dependent adjoint solutions for the case study by using the continuous adjoint method. The advantages of calculating the time-dependent adjoint fluxes by solving time-dependent adjoint systems are also discussed in this section. Section IV presents the discrete adjoint method and the calculation of the time-dependent adjoint solutions by using the discrete adjoint method, which further verifies the continuous adjoint fluxes. The pros and cons of the discrete adjoint method are briefly discussed. The computational equivalence of both methods is also demonstrated and discussed in this section. Section V summarizes the work and offers some conclusions about the two adjoint methods based on the study's findings.

II. CASE STUDY

A rod ejection accident (REA) is one of the reactivity initiated accidents (RIA) in which a large amount of reactivity is inserted into the reactor core during a short period. REA is an ideal transient to be studied for time-dependent adjoint solutions because of the rapid and intense changes in both neutron fluxes and DNP concentrations. We selected the postulated REA investigated by Vidal-Ferràndiz et al.[31] as the case study in this work such that our steady-state solutions and forward transient solutions were verified to demonstrate the correctness of our forward system. This also provided a solid base for the adjoint transient calculations performed in the sections thereafter.

II.A. Problem Description

A detailed description of the postulated REA can be found in Ref. 31 but is briefly summarized in this section such that readers can understand the case study without referring to external references. The simplified one-dimensional (1-D) reactor, in which the postulated REA took place, consisted of 12 cells of 25 cm each. This indicates that the total height of the reactor was 300 cm. The cells in the reactor were formed by different materials and were categorized into "Reflector," "Unrodded fuel," and "Rodded fuel," accordingly. The control rod was inserted to 125 cm from the bottom of the reactor before initiation of the transient. During the 10-s transient, the control rod was ejected from the top of the reactor with a constant velocity of 25 cm/s from 0 to 4s and inserted back into the reactor from 4 to 10s with a constant velocity of 25 cm/s. The geometry of the simplified 1-D reactor during the transient is shown in Fig. 1. Both the steady-state and the transient calculations were conducted by solving the two-group diffusion equations established for the problem. The velocity of the fast group (group 1) neutrons was assumed to be $v_1 = 1.27 \times 10^7$ cm/s while that of the thermal group (group 2) neutrons was assumed to be $v_2 = 2.50 \times 10^5$cm/s. The two-group cross sections of cells of different categories are summarized in Table I. Six families of DNPs were considered in this study, and their parameters are summarized in Table II.

II.B. Steady-State Calculations

We first solved the following steady-state two-group diffusion equations to calculate the dominant eigenvalue k_{eff} of the simplified 1-D reactor before initiation of the transient calculations:

$$\begin{cases} -\frac{d}{dx}\left(D_1 \frac{d\phi_1}{dx}\right) + \Sigma_{r,1}\phi_1 = \frac{1}{k_{eff}}\left(\nu\Sigma_{f,1}\phi_1 + \nu\Sigma_{f,2}\phi_2\right) \\ -\frac{d}{dx}\left(D_2 \frac{d\phi_2}{dx}\right) + \Sigma_{a,2}\phi_2 = \Sigma_{s,1\to 2}\phi_1 \end{cases}, \quad (1)$$

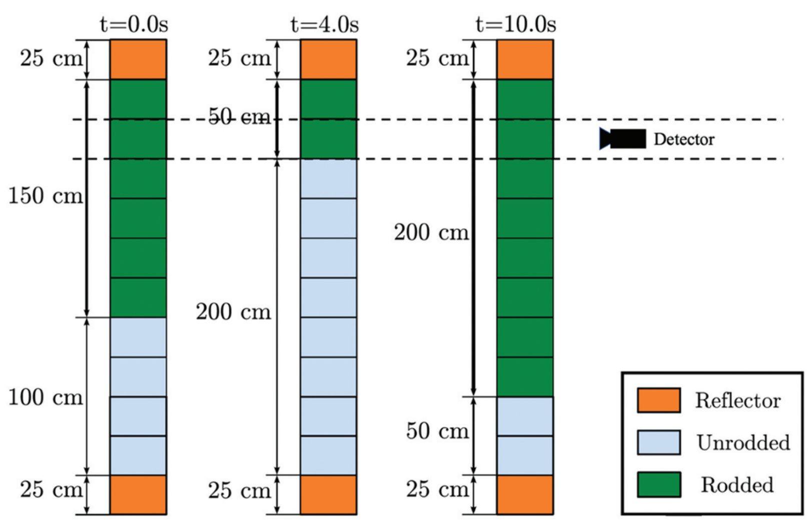

Fig. 1. Geometry of the 1-D reactor during the postulated REA (Ref. 31).

TABLE I

Cross Sections of Cells of Different Categories in the 1-D Reactor*

	Group 1				Group 2		
	D_1 (cm)	$\Sigma_{a,1}\left(\mathrm{cm}^{-1}\right)$	$\nu\Sigma_{f,1}$ $\left(\mathrm{cm}^{-1}\right)$	$\Sigma_{s,1\to 2}$ $\left(\mathrm{cm}^{-1}\right)$	D_2 (cm)	$\Sigma_{a,2}\left(\mathrm{cm}^{-1}\right)$	$\nu\Sigma_{f,2}$ $\left(\mathrm{cm}^{-1}\right)$
Unrodded fuel	1.40343	1.17659e-2	5.62285e-3	1.60795e-2	0.32886	1.07186e-1	1.45865e-1
Rodded fuel	1.40343	1.17659e-2	5.60285e-3	1.60795e-2	0.32886	1.07186e-1	1.45403e-1
Reflector	0.93344	2.81676e-3	0	1.08805e-2	0.95793	8.87200e-2	0

*Reference 31.

TABLE II

DNP Parameters in the 1-D Reactor*

	Family 1	Family 2	Family 3	Family 4	Family 5	Family 6
β_i	0.000247	0.0013845	0.001222	0.026455	0.000832	0.000169
λ_i $\left(\mathrm{s}^{-1}\right)$	0.0127	0.0317	0.115	0.311	1.4	3.87

*Reference 31.

where

g = 1, 2

ϕ_g = flux

D_g = diffusion coefficient

$\Sigma_{a,g}$ = macroscopic absorption cross section

$\Sigma_{f,g}$ = macroscopic fission cross section of the group g neutrons

$\Sigma_{s,1\to 2}$ = macroscopic downscattering cross section of the fast group neutrons

$\Sigma_{r,1} = \Sigma_{a,1} + \Sigma_{s,1\to 2}$.

Similar to those employed in Ref. 31, the zero-current boundary conditions (i.e., reflective conditions) were imposed at the boundaries of the system.

By noting $\boldsymbol{\phi} = (\phi_1 \quad \phi_2)^T$, Eq. (1) can also be expressed in matrix form as

$$\boldsymbol{L}\phi = \boldsymbol{0}\,, \tag{2}$$

where $\boldsymbol{L}$ is the two-group diffusion operator of the simplified 1-D reactor with the expression of

$$\boldsymbol{L} = \begin{pmatrix} -\frac{d}{dx}\left(D_1\frac{d}{dx}\right) + \Sigma_{r,1} - \frac{1}{k_{eff}}\nu\Sigma_{f,1} & -\frac{1}{k_{eff}}\nu\Sigma_{f,2} \\ -\Sigma_{s,1\to 2} & -\frac{d}{dx}\left(D_2\frac{d}{dx}\right) + \Sigma_{a,2} \end{pmatrix}. \tag{3}$$

For the numerical implementation, a uniform-mesh-size spatial discretization of Eq. (2) was adopted to calculate k_{eff}. Macroscopic cross sections Σ and diffusion coefficients D were defined at the mesh centers, as depicted in Fig. 2. The second-order spatial derivative $\frac{\partial}{\partial x}\left(D\frac{\partial}{\partial x}\right)$

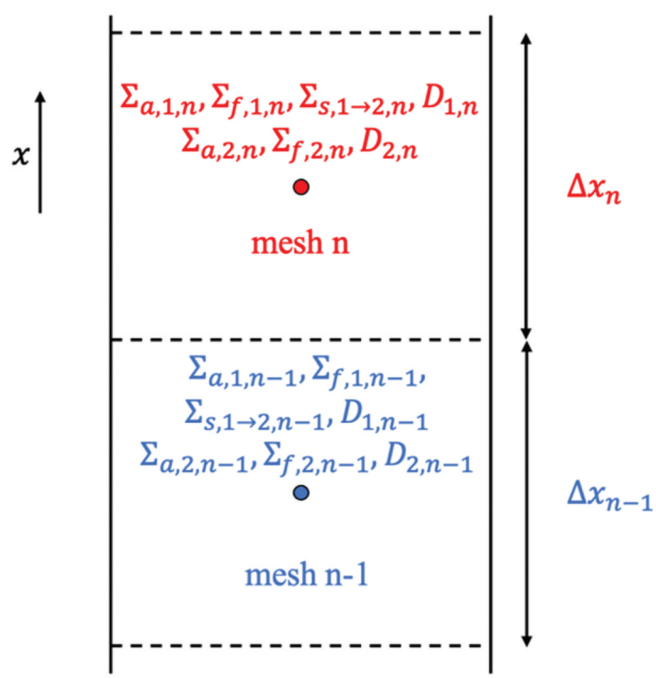

Fig. 2. Uniform-mesh-size spatial discretization scheme employed for the solution of two-group diffusion equations.

terms were approximated by the center-difference scheme.

We are interested in the steady-state solutions as these solutions would provide a reasonable initial condition for the transients, but we omitted the detailed calculation procedure for the steady-state case here as it was regarded as fairly common practice and has already been widely discussed.[31,32] However, it is worthy of pointing out that the correctly calculated k_{eff} makes the operator $\boldsymbol{L}$ noninvertible because $\boldsymbol{L}\phi = \boldsymbol{0}$ has nontrivial solutions for ϕ, which means $det(\boldsymbol{L}) = 0$. Also, when the k_{eff} is correctly calculated, ϕ will have infinitely many solutions as long as they stay in the null space of $\boldsymbol{L}$. The corresponding physical explanation to this phenomenon is that the reactor can remain self-sustainingly critical at any power level. By employing a uniform mesh size Δx of 5 cm, we found that $k_{eff} = 0.97890$ for the case problem whereas the reference k_{eff} provided in Ref. 31 was 0.97881. The difference between the k_{eff} obtained in both works was only 9 per cent mille (pcm), which indicates the steady-state two-group diffusion equations were correctly solved.

Last, before moving to the transient calculations, we adjusted the fission macroscopic cross sections ($\Sigma_{f,1}$ and $\Sigma_{f,2}$) by the factor of $1/k_{eff}$ in all the following transient calculations to make sure that the postulated REA was initiated from a steady state. The spatial discretization scheme employed in the steady-state calculations was also employed in all the following transient calculations.

II.C. Forward Transient Calculations

We modified Eq. (1) by adding time-dependent and DNP-related terms to calculate the time-dependent flux distributions. One equation for each of the six groups of DNPs was also added to the system to track the changes in DNP concentrations. By noting $\beta_{tot} = \sum_{i=1}^{6} \beta_i$, the forward transient equations were developed as

$$\begin{cases} \dfrac{1}{v_1}\dfrac{\phi_1}{\partial t} - \dfrac{\partial}{\partial x}\left(D_1 \dfrac{\partial \phi_1}{\partial x}\right) + \Sigma_{r,1}\phi_1 = (1-\beta_{tot})\left(\nu\Sigma_{f,1}\phi_1 + \nu\Sigma_{f,2}\phi_2\right) + \displaystyle\sum_{k=1}^{6}\lambda_i C_i \\ \dfrac{1}{v_2}\dfrac{\partial \phi_2}{\partial t} - \dfrac{\partial}{\partial x}\left(D_2 \dfrac{\partial \phi_2}{\partial x}\right) + \Sigma_{a,2}\phi_2 = \Sigma_{s,1\to 2}\phi_1 \\ \dfrac{\partial C_i}{\partial t} = \beta_i\left(\nu\Sigma_{f,1}\phi_1 + \nu\Sigma_{f,2}\phi_2\right) - \lambda_i C_i \qquad (i = 1 \text{ to } 6) \end{cases} , \tag{4}$$

where C_i and λ_i stand for the concentration and the decay constant of the family-i DNP and β_i stands for the fractional yield of delayed neutrons from the family-i DNP. For neutron equations, the zero-current boundary conditions were imposed at the boundaries of the system during the entire transient, and the initial conditions were prescribed as the steady-state flux calculated in Sec. II.B. For DNP concentration equations, the initial conditions were calculated accordingly from the steady-state flux solutions:

$$C_i = \frac{\beta_i}{\lambda_i}\left(\nu\Sigma_{f,1}\phi_1 + \nu\Sigma_{f,2}\phi_2\right) \qquad (i = 1 \text{ to } 6). \tag{5}$$

By using an implicit time discretization scheme for the time variable and standard difference form–based discretization scheme for the spatial variable, with the boundary and initial conditions described above, the discretized forms of Eq. (4) can be expressed by Eqs. (6) through (13) as follows, considering two energy groups of neutron flux and six families of DNP concentrations:

$$\begin{aligned} \mathbb{N}_{1,n}^{m} := {} & A_{1,n,n-1}^{m}\phi_{1,n-1}^{m} + A_{1,n,n}^{m}\phi_{1,n}^{m} + A_{1,n,n+1}^{m}\phi_{1,n+1}^{m} + B_{1,n,n}^{m}\phi_{2,n}^{m} + D_{1,n,n}^{m}C_{1,n}^{m} \\ & + E_{1,n,n}^{m}C_{2,n}^{m} + F_{1,n,n}^{m}C_{3,n}^{m} + G_{1,n,n}^{m}C_{4,n}^{m} + H_{1,n,n}^{m}C_{5,n}^{m} + L_{1,n,n}^{m}C_{6,n}^{m} \\ & + K_{1,n,n}^{m}\phi_{1,n}^{m-1} = 0 \ , \end{aligned} \tag{6}$$

$$\mathbb{N}_{2,n}^{m} := A_{2,n,n}^{m}\phi_{1,n}^{m} + B_{2,n,n-1}^{m}\phi_{2,n-1}^{m} + B_{2,n,n}^{m}\phi_{2,n}^{m} + B_{2,n,n+1}^{m}\phi_{2,n+1}^{m} + K_{2,n,n}^{m}\phi_{2,n}^{m-1} = 0 \ , \tag{7}$$

$$\mathbb{N}_{3,n}^{m} := A_{3,n,n}^{m}\phi_{1,n}^{m} + B_{3,n,n}^{m}\phi_{2,n}^{m} + D_{3,n,n}^{m}C_{1,n}^{m} + K_{3,n,n}^{m}C_{1,n}^{m-1} = 0 \ , \tag{8}$$

$$\mathbb{N}_{4,n}^{m} := A_{4,n,n}^{m}\phi_{1,n}^{m} + B_{4,n,n}^{m}\phi_{2,n}^{m} + E_{4,n,n}^{m}C_{2,n}^{m} + K_{4,n,n}^{m}C_{2,n}^{m-1} = 0 \ , \tag{9}$$

$$\mathbb{N}_{5,n}^{m} := A_{5,n,n}^{m}\phi_{1,n}^{m} + B_{5,n,n}^{m}\phi_{2,n}^{m} + F_{5,n,n}^{m}C_{3,n}^{m} + K_{5,n,n}^{m}C_{3,n}^{m-1} = 0 \ , \tag{10}$$

$$\mathbb{N}_{6,n}^{m} := A_{6,n,n}^{m}\phi_{1,n}^{m} + B_{6,n,n}^{m}\phi_{2,n}^{m} + G_{6,n,n}^{m}C_{4,n}^{m} + K_{6,n,n}^{m}C_{4,n}^{m-1} = 0 \ , \tag{11}$$

$$\mathbb{N}_{7,n}^{m} := A_{7,n,n}^{m}\phi_{1,n}^{m} + B_{7,n,n}^{m}\phi_{2,n}^{m} + H_{7,n,n}^{m}C_{5,n}^{m} + K_{7,n,n}^{m}C_{5,n}^{m-1} = 0 \ , \tag{12}$$

and

$$\mathbb{N}_{8,n}^{m} := A_{8,n,n}^{m}\phi_{1,n}^{m} + B_{8,n,n}^{m}\phi_{2,n}^{m} + L_{8,n,n}^{m}C_{6,n}^{m} + K_{8,n,n}^{m}C_{6,n}^{m-1} = 0 \ . \tag{13}$$

In Eqs. (6) through (13), the subscript $n \in [1, N]$ represents the mesh of interest, where we set $N = 60$ as we employed a uniform mesh size Δx of 5 cm while the simplified 1-D reactor had a total height of 300 cm. The superscript $m \in [1, M]$ represents the time step of interest, where we set $M = 20$ as we employed a uniform time step $\Delta t = 0.5\text{s}$ while the entire transient of interest lasted for 10s. The coefficients $(A, B, D, E, F, G, H, K, L, \text{and}\, K)$ occurring in Eqs. (6) through (13) may vary with different numerical discretization methods. The coefficients used in this study are detailed in Eqs. (A.1) through (A.40) in the Appendix. It is also to be noted that Eqs. (6) through (13) are all written with a leading term $\mathbb{N} :=$, which basically defines the equations. Here, $\mathbb{N}$ can be considered as a residual form of each equation. We purposely write the discrete equation into such a form as it will greatly facilitate the introduction of the discrete adjoint method described in Sec. IV.

By writing Eqs. (6) through (13) in matrix form, the flux and DNP concentrations at time step m are calculated from those at time step $m - 1$ by solving

$$\mathcal{M}^{\boldsymbol{m}}\phi^{\boldsymbol{m}} = \boldsymbol{K}^{\boldsymbol{m}}\phi^{\boldsymbol{m-1}} \, , \tag{14}$$

where

$$\mathcal{M}^{m} = \begin{pmatrix} \boldsymbol{A_1^m} & \boldsymbol{B_1^m} & \boldsymbol{D_1^m} & \boldsymbol{E_1^m} & \boldsymbol{F_1^m} & \boldsymbol{G_1^m} & \boldsymbol{H_1^m} & \boldsymbol{L_1^m} \\ \boldsymbol{A_2^m} & \boldsymbol{B_2^m} & \boldsymbol{0} & \cdots & \cdots & \cdots & \cdots & \boldsymbol{0} \\ \boldsymbol{A_3^m} & \boldsymbol{B_3^m} & \boldsymbol{D_3^m} & \ddots & & & & \vdots \\ \boldsymbol{A_4^m} & \boldsymbol{B_4^m} & \boldsymbol{0} & \boldsymbol{E_4^m} & \ddots & & & \vdots \\ \boldsymbol{A_5^m} & \boldsymbol{B_5^m} & \vdots & \ddots & \boldsymbol{F_5^m} & \ddots & & \vdots \\ \boldsymbol{A_6^m} & \boldsymbol{B_6^m} & \vdots & & \ddots & \boldsymbol{G_6^m} & \ddots & \vdots \\ \boldsymbol{A_7^m} & \boldsymbol{B_7^m} & \vdots & & & \ddots & \boldsymbol{H_7^m} & \boldsymbol{0} \\ \boldsymbol{A_8^m} & \boldsymbol{B_8^m} & \boldsymbol{0} & \cdots & \cdots & \cdots & \boldsymbol{0} & \boldsymbol{L_8^m} \end{pmatrix}_{\in(8N,8N)} \, , \tag{15}$$

$$K^m = \begin{pmatrix} K_1^m & 0 & \cdots & \cdots & \cdots & \cdots & \cdots & 0 \\ 0 & K_2^m & \ddots & & & & & \vdots \\ \vdots & \ddots & K_3^m & \ddots & & & & \vdots \\ \vdots & & \ddots & K_4^m & \ddots & & & \vdots \\ \vdots & & & \ddots & K_5^m & \ddots & & \vdots \\ \vdots & & & & \ddots & K_6^m & \ddots & \vdots \\ \vdots & & & & & \ddots & K_7^m & 0 \\ 0 & \cdots & \cdots & \cdots & \cdots & \cdots & 0 & K_8^m \end{pmatrix}_{\in(8N,8N)} , \tag{16}$$

and

$$\phi^m = \begin{pmatrix} \phi_1^m \\ \phi_2^m \\ C_1^m \\ C_2^m \\ C_3^m \\ C_4^m \\ C_5^m \\ C_6^m \end{pmatrix}_{\in(8N,1)} . \tag{17}$$

All the submatrices in Eqs. (15) and (16) are diagonal (N, N) matrices except A_1^m and B_2^m, which are tridiagonal. The submatrices in Eq. (17) are $(N, 1)$ vectors representing the distributions of neutron flux and DNP concentrations at time step m of the transient. Detailed expression of the submatrices of Eqs. (15), (16), and (17) can be found in Eqs. (A.41) through (A.59) in the Appendix. The initial condition is expressed as ϕ^0, which consists of the steady-state two-group fluxes and DNP concentrations calculated in Sec. II.B.

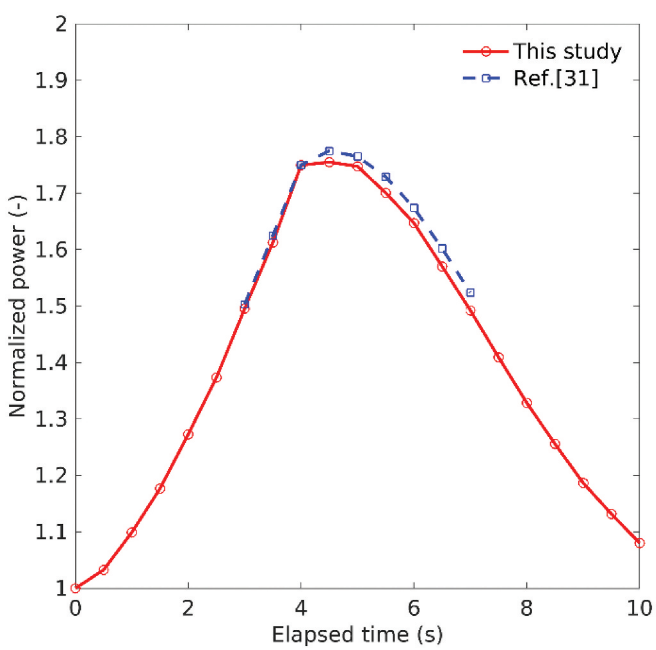

Fig. 3. Comparison of the normalized power obtained in this study with that from Ref. 31.

By varying m from 1 to M and recurrently solving Eq. (14), we obtained the time-dependent solutions of the neutron flux and the DNP concentrations. We quantified the normalized mean power by using

$$P^m = \frac{\sum_{n=1}^{N} \left(\nu\Sigma_{f,1,n}^m \phi_{1,n}^m \Delta x_n + \nu\Sigma_{f,2,n}^m \phi_{2,n}^m \Delta x_n \right)}{\sum_{n=1}^{N} \left(\nu\Sigma_{f,1,n}^0 \phi_{1,n}^0 \Delta x_n + \nu\Sigma_{f,2,n}^0 \phi_{2,n}^0 \Delta x_n \right)} . \tag{18}$$

The normalized mean power during the transient is plotted as a function of the elapsed time in Fig. 3 in comparison with that provided in Ref. 31. The maximum relative difference was around 2%, which demonstrated the forward transient solutions established in this work to be correct and the choices of both Δx and Δt to be appropriate. The discrepancy that exists in the power prediction, particularly for the larger ones that appeared after 4 s, is mainly attributed to the limited modeling capabilities of the uniform mesh definition for the case problem. This limitation is clearly explained in Ref. 31. Since the primary goal of this study is to explore the adjoint calculations using this case problem, investigating and reducing the discrepancies appearing in Fig. 3 are out of the work scope of the paper.

The time-dependent distributions of the fast group neutron flux ϕ_1, the thermal group neutron flux ϕ_2, and the first-family DNP concentration C_1, at time step $m = 4, 8, 12, 16, \text{and} \, 20$ (2, 4, 6, 8, and 10 s into the transient) are plotted in Fig. 4. Because of the small decay constants, the magnitudes of the DNP concentrations are less sensitive to the control rod movement than those of the neutron fluxes. All the three distributions peaked around the middle of the 1-D reactor in Fig. 4, while neutron flux distributions were more dependent on the control rod location. The more the rod was inserted, the more the peaks of the flux distributions would move to the lower part of the 1-D reactor, as observed by comparing ϕ_1 and ϕ_2 distributions at 4 and 6 s. On the contrary, the neutron flux and DNP distributions were independent of the location of the detector.

III. ADJOINT TRANSIENT CALCULATIONS WITH THE CONTINUOUS ADJOINT METHOD

Starting with this section, we investigate the transient (i.e., time-dependent) adjoint solutions in the simplified 1-D reactor through the adjoint transient calculations via two distinct numerical approaches. The continuous adjoint method is discussed and employed in Sec. III.A while the application of the discrete adjoint method is deferred to Sec. III.B.

III.A. Continuous Adjoint Method

Since the adjoint solutions are always associated with a specific response in the forward system, the quantity of interest (QOI) as a general response is required to be defined first for the adjoint system. As described earlier, a neutron detector was positioned in the third cell from the top of the 1-D reactor during the postulated REA (see Fig. 1). The reading of the detector was selected as the QOI in this study, and the response was therefore expressed as the reaction rate density (in $s^{-1} \cdot cm^{-3}$) described as

$$R(t) = \Sigma_{d,1}\phi_1(t) + \Sigma_{d,2}\phi_2(t) , \tag{19}$$

where $\Sigma_{d,1}$ and $\Sigma_{d,2}$ are the equivalent macroscopic detector cross sections in the simplified 1-D reactor (the reactor is not responsive to DNP). $\Sigma_{d,1}$ and $\Sigma_{d,2}$ are assumed to be 0.2 cm^{-1} and 0.02 cm^{-1} in this study. The corresponding adjoint solutions are first calculated with the continuous adjoint method in this section.

As the adjoint operator is essentially the transpose of the forward operator in neutron diffusion equations,[33] the adjoint system of the simplified 1-D reactor is derived from Eq. (4) as

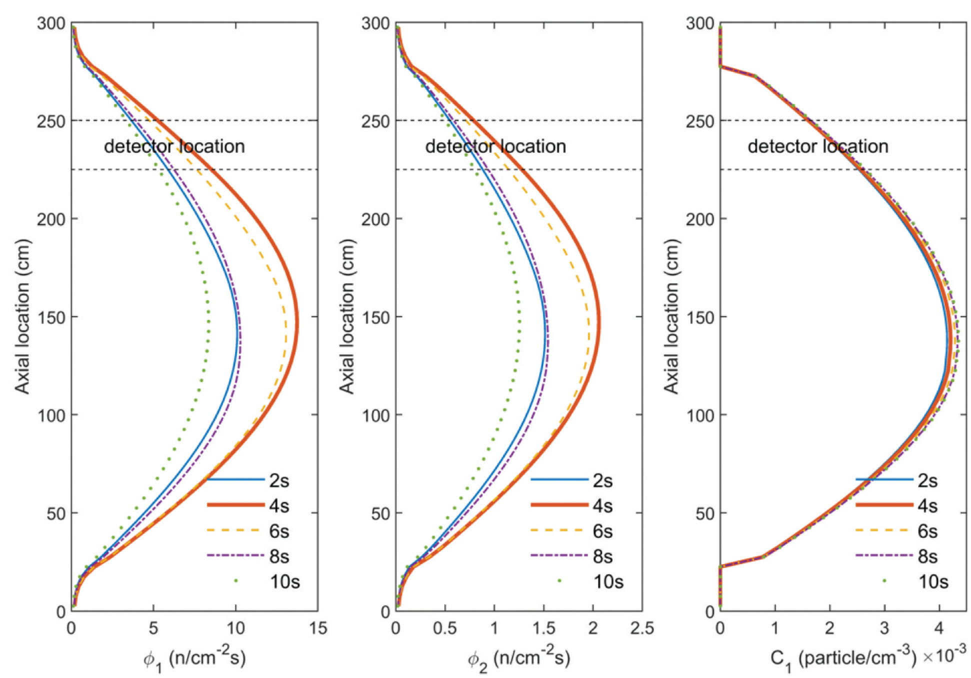

Fig. 4. Comparison of time-dependent distributions of ϕ_1, ϕ_2, and C_1.

$$\begin{cases} -\frac{1}{v_1}\frac{\partial \phi_1^*}{\partial t} - \frac{\partial}{\partial x}\left(D_1 \frac{\partial \phi_1^*}{\partial x}\right) + \Sigma_{r,1}\phi_1^* = (1-\beta_{tot})\nu\Sigma_{f,1}\phi_1^* + \Sigma_{s,1\to 2}\phi_2^* + \sum_{k=i}^{6}\beta_i\nu\Sigma_{f,1}C_i^* \\ -\frac{1}{v_2}\frac{\partial \phi_2^*}{\partial t} - \frac{\partial}{\partial x}\left(D_2 \frac{\partial \phi_2^*}{\partial x}\right) + \Sigma_{a,2}\phi_2^* = (1-\beta_{tot})\nu\Sigma_{f,2}\phi_1^* \\ + \sum_{i=1}^{6}\beta_i\nu\Sigma_{f,2}C_i^* - \frac{\partial C_i^*}{\partial t} = \lambda_i\phi_1^* - \lambda_i C_i (i = 1 \text{ to } 6)\ , \end{cases} \tag{20}$$

where ϕ_1^*, ϕ_2^*, and C_i^* are the adjoint solutions of ϕ_1, ϕ_2, and C_i, respectively. To be consistent with the zero-current boundary conditions for the forward equations, a zero adjoint solution gradient was imposed as the boundary condition for the adjoint system. As a backward problem, the final state condition for the adjoint system is to set the adjoint solutions (including the adjoint fluxes and adjoint DNP concentrations) as all zero. The physical explanation for this consideration is that the detector was hypothetically removed at the end of the transient (at time step M), and the flux in the reactor did not impact the readings of the detector at any time after time step M. The importance of neutrons and DNP with respect to the readings of the detector therefore became zero, as well as the corresponding adjoint solutions.

We discretized Eq. (20) by using an implicit time discretization scheme and the spatial discretization scheme described in Sec. II.B. Following the similar pattern as the forward transient calculations, the discretized form of Eq. (20) can be expressed by Eqs. (21) through (28) as follows (eight equations in total):

$$\begin{aligned} &A^{*m}_{1,n,n-1}\phi^{*m}_{1,n-1} + A^{*m}_{1,n,n}\phi^{*m}_{1,n} + A^{*m}_{1,n,n+1}\phi^{*m}_{1,n+1} \\ &+ B^{*m}_{1,n,n}\phi^{*m}_{2,n} + D^{*m}_{1,n,n}C^{*m}_{1,n} + E^{*m}_{1,n,n}C^{*m}_{2,n} \\ &+ F^{*m}_{1,n,n}C^{*m}_{3,n} + G^{*m}_{1,n,n}C^{*m}_{4,n} + H^{*m}_{1,n,n}C^{*m}_{5,n} \\ &+ L^{*m}_{1,n,n}C^{*m}_{6,n} + K^{*m}_{1,n,n}\phi^{*m+1}_{1,n} = 0\ , \end{aligned} \tag{21}$$

$$\begin{aligned} &A^{*m}_{2,n,n}\phi^{*m}_{1,n} + B^{*m}_{2,n,n-1}\phi^{*m}_{2,n-1} + B^{*m}_{2,n,n}\phi^{*m}_{2,n} \\ &+ B^{*m}_{2,n,n+1}\phi^{*m}_{2,n+1} + D^{*m}_{2,n,n}C^{*m}_{1,n} + E^{*m}_{2,n,n}C^{*m}_{2,n} \\ &+ F^{*m}_{2,n,n}C^{*m}_{3,n} + G^{*m}_{2,n,n}C^{*m}_{4,n} + H^{*m}_{2,n,n}C^{*m}_{5,n} \\ &+ L^{*m}_{2,n,n}C^{*m}_{6,n} + K^{*m}_{2,n,n}\phi^{*m+1}_{2,n} = 0\ , \end{aligned} \tag{22}$$

$$A^{*m}_{3,n,n}\phi^{*m}_{1,n} + D^{*m}_{3,n,n}C^{*m}_{1,n} + K^{*m}_{3,n,n}C^{*m+1}_{1,n} = 0\ , \tag{23}$$

$$A^{*m}_{4,n,n}\phi^{*m}_{1,n} + E^{*m}_{4,n,n}C^{*m}_{2,n} + K^{*m}_{4,n,n}C^{*m+1}_{2,n} = 0\ , \tag{24}$$

$$A^{*m}_{5,n,n}\phi^{*m}_{1,n} + F^{*m}_{5,n,n}C^{*m}_{3,n} + K^{*m}_{5,n,n}C^{*m+1}_{3,n} = 0\ , \tag{25}$$

$$A^{*m}_{6,n,n}\phi^{*m}_{1,n} + G^{*m}_{6,n,n}C^{*m}_{4,n} + K^{*m}_{6,n,n}C^{*m+1}_{4,n} = 0\ , \tag{26}$$

$$A^{*m}_{7,n,n}\phi^{*m}_{1,n} + H^{*m}_{7,n,n}C^{*m}_{5,n} + K^{*m}_{7,n,n}C^{*m+1}_{5,n} = 0\ , \tag{27}$$

and

$$A^{*m}_{8,n,n}\phi^{m}_{1,n} + L^{*m}_{8,n,n}C^{*m}_{6,n} + K^{*m}_{8,n,n}C^{*m+1}_{6,n} = 0. \tag{28}$$

Similar to Eqs. (6) through (13), the subscript $n \in [1,N]$ represents the mesh of interest, and the superscript $m \in [1,M]$ represents the time step of interest in Eqs. (21) through (28). The coefficients occurring in Eqs. (21) through (28) are detailed in Eqs. (A.60) through (A.99) in the Appendix. It is noted that the adjoint system is a backward system,[22,23,30] and the adjoint solutions are solved backwards in time ($\phi^{*M} \to \phi^{*M-1} \to \ldots \to \phi^{*1}$). The implicit time discretization for the adjoint systems therefore resembles the explicit time discretization for the forward systems. As discussed above, the final condition adopted in this study was that the adjoint solutions at time step $M+1$ are all zero ($\phi^{*M+1}_{1,n}$, $\phi^{*M+1}_{2,n}$, and $C^{*M+1}_{1,n} \sim C^{*M+1}_{6,n} = 0$ for any $n \in [1,N]$).

By rewriting Eqs. (21) through (28) in matrix form, we obtain

$$\mathcal{M}^*\phi^* = \mathbf{0}\ , \tag{29}$$

where

$$\mathcal{M}^* = \begin{pmatrix} \mathcal{M}^{*1} & \boldsymbol{K}^{*1} & \mathbf{0} & \cdots & \cdots & \cdots & \mathbf{0} \\ \mathbf{0} & \mathcal{M}^{*2} & \boldsymbol{K}^{*2} & \mathbf{0} & & & \vdots \\ \mathbf{0} & \mathbf{0} & \mathcal{M}^{*3} & \boldsymbol{K}^{*3} & \mathbf{0} & & \vdots \\ \vdots & & \ddots & \ddots & \ddots & \ddots & \vdots \\ \vdots & & & \mathbf{0} & \mathcal{M}^{*M-2} & \boldsymbol{K}^{*M-2} & \mathbf{0} \\ \vdots & & & & \mathbf{0} & \mathcal{M}^{*M-1} & \boldsymbol{K}^{*M-1} \\ \mathbf{0} & \cdots & \cdots & \cdots & \cdots & \mathbf{0} & \mathcal{M}^{*M} \end{pmatrix}_{\in(8NM,8NM)} , \tag{30}$$

$$\mathcal{M}^{*m} = \begin{pmatrix} \boldsymbol{A}^{*m}_1 & \boldsymbol{B}^{*m}_1 & \boldsymbol{D}^{*m}_1 & \boldsymbol{E}^{*m}_1 & \boldsymbol{F}^{*m}_1 & \boldsymbol{G}^{*m}_1 & \boldsymbol{H}^{*m}_1 & \boldsymbol{L}^{*m}_1 \\ \boldsymbol{A}^{*m}_2 & \boldsymbol{B}^{*m}_2 & \boldsymbol{D}^{*m}_2 & \boldsymbol{E}^{*m}_2 & \boldsymbol{F}^{*m}_2 & \boldsymbol{G}^{*m}_1 & \boldsymbol{H}^{*m}_2 & \boldsymbol{L}^{*m}_2 \\ \boldsymbol{A}^{*m}_3 & \mathbf{0} & \boldsymbol{D}^{*m}_3 & \ddots & & & & \vdots \\ \boldsymbol{A}^{*m}_4 & \vdots & \ddots & \boldsymbol{E}^{*m}_4 & \ddots & & & \vdots \\ \boldsymbol{A}^{*m}_5 & \vdots & & \ddots & \boldsymbol{F}^{*m}_5 & \ddots & & \vdots \\ \boldsymbol{A}^{*m}_6 & \vdots & & & \ddots & \boldsymbol{G}^{*m}_6 & \ddots & \vdots \\ \boldsymbol{A}^{*m}_7 & \vdots & & & & \ddots & \boldsymbol{H}^{*m}_7 & \mathbf{0} \\ \boldsymbol{A}^{*m}_8 & \mathbf{0} & \cdots & \cdots & \cdots & \cdots & \mathbf{0} & \boldsymbol{L}^{*m}_8 \end{pmatrix}_{\in(8N,8N)} , \tag{31}$$

and

$$\boldsymbol{K}^{*m} = \begin{pmatrix} \boldsymbol{K}^{*m}_1 & \mathbf{0} & \cdots & \cdots & \cdots & \cdots & \cdots & \mathbf{0} \\ \mathbf{0} & \boldsymbol{K}^{*m}_2 & \ddots & & & & & \vdots \\ \vdots & \ddots & \boldsymbol{K}^{*m}_3 & \ddots & & & & \vdots \\ \vdots & & \ddots & \boldsymbol{K}^{*m}_4 & \ddots & & & \vdots \\ \vdots & & & \ddots & \boldsymbol{K}^{*m}_5 & \ddots & & \vdots \\ \vdots & & & & \ddots & \boldsymbol{K}^{*m}_6 & \ddots & \vdots \\ \vdots & & & & & \ddots & \boldsymbol{K}^{*m}_7 & \mathbf{0} \\ \mathbf{0} & \cdots & \cdots & \cdots & \cdots & \cdots & \mathbf{0} & \boldsymbol{K}^{*m}_8 \end{pmatrix}_{\in(8N,8N)} . \tag{32}$$

All the submatrices in Eqs. (31) and (32) are diagonal (N,N) matrices except $\boldsymbol{A}^{*m}_1$ and $\boldsymbol{B}^{*m}_2$, which are tridiagonal. Detailed expression of the submatrices of Eqs. (31) and (32) can be found in Eqs. (A.100) through (A.110) in the Appendix.

The corresponding adjoint source is added to the right-hand side of Eq. (29) to calculate the adjoint fluxes (importance of neutrons and DNP) to a specific QOI (Ref. 33). In the case where the detector readings are considered as the QOI, the adjoint source is the equivalent detector cross section.[33] When the detector readings at a specific moment in time t_0 are of interest, the adjoint source should be further multiplied by the term $\delta(t-t_0)$ (Ref. 18). Therefore, the time-dependent adjoint solutions to the detector readings at time step m ($m \in [1,M]$) can be obtained by solving

$$\mathcal{M}^*\phi^{*m} = -\boldsymbol{S}^{*m} , \tag{33}$$

where

$$\phi^{*m} = \begin{pmatrix} \phi^{*m,1} \\ \phi^{*m,2} \\ \vdots \\ \phi^{*m,M} \end{pmatrix}_{\in(8NM,1)} \tag{34}$$

and

$$\boldsymbol{S}^{*m} = \begin{pmatrix} \mathbf{0} \\ \vdots \\ \mathbf{0} \\ \boldsymbol{S}^{*m,m} \\ \mathbf{0} \\ \vdots \\ \mathbf{0} \end{pmatrix}_{\in(8NM,1)} . \tag{35}$$

The submatrices of ϕ^{*m}, namely, $\phi^{*m,i}$ $(i \in [1, M])$, are $(8N, 1)$ vectors that represent the importance of the neutrons and DNP at time step i to the detector readings at time step m. Because the detector was installed at the third cell from the top of the 1-D reactor and each cell was modeled with five meshes, the meaningful vector $\boldsymbol{S}^{*m,m}$ can be expressed as

$$\boldsymbol{S}^{*m,m}(j) = \begin{cases} \Sigma_{d,1} \text{ if } j \in [p(I_d - 1) + 1, pI_d] \\ \Sigma_{d,2} \text{ if } j \in [p(I_d - 1) + 1 + N, pI_d + N] \\ 0 \text{ if else} \end{cases} , \tag{36}$$

where p is the number of meshes per cell (5 in the example case), I_d is the number of the cell in which the detector is located (3 in this example case), and N is the total mesh number (60 in this example case). With all the matrices and vectors in Eq. (33) straightened as above, we can obtain the time-dependent adjoint solutions by varying m from 1 to M and recurrently solving Eq. (33).

III.B. Transient Adjoint Solutions by the Continuous Adjoint Method

The time-dependent continuous adjoint solutions of the fast group neutron flux $\phi_1^{*m,i}$, the thermal group neutron flux $\phi_2^{*m,i}$, and the first-family DNP concentration $\boldsymbol{C}_1^{*m,i}$ to the detector readings at the time step $m = 10$ (5 s into the transient) are plotted in Fig. 5. Both the fast group and the thermal group adjoint fluxes peaked at the location of the detector, which suggests that unlike the flux distributions that were independent of the detector location, the importance of the neutrons to the detector response increased when being closer to the location of the detector. In addition, both $\phi_1^{*m,i}$ and $\phi_2^{*m,i}$ became zero when $i > m$ because the future variations in neutron flux did not affect the current readings of the detector, which makes physical sense. On the other hand, $\phi_1^{*m,i}$ and $\phi_2^{*m,i}$ were not zero when $i < m$ because the past variations in neutron flux could affect the current readings of the detector, which also makes physical sense, as it suggests that although the detector was not directly responsive to the neutron flux in the past, the latter had an impact on the current neutron flux that further affected current readings of the detector.

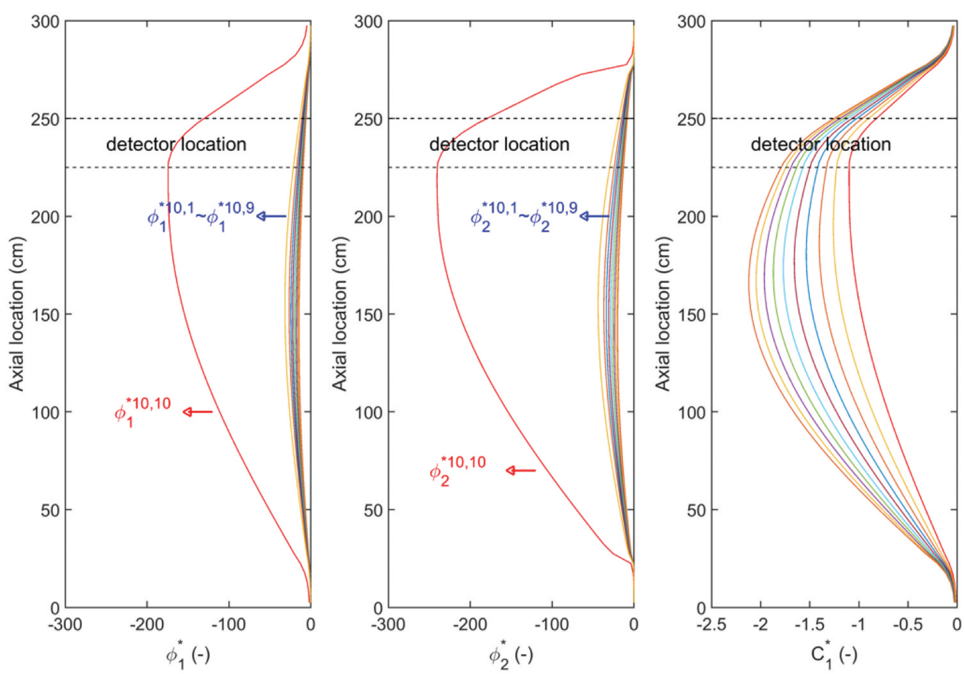

Fig. 5. Time-dependent continuous adjoint solutions to the detector readings at 5 s.

However, the importance of the neutrons in the past was more than one order of magnitude smaller than that of the current one (for the time step size employed in this study). Moreover, because of the small fractional yield of delayed neutrons, the importance of the DNP to the detector was more than two orders of magnitude smaller than that of the neutron flux.

The current-time continuous adjoint solutions of the fast group neutron flux $\phi_1^{*m,m}$, the thermal group neutron flux $\phi_2^{*m,m}$, and the first-family DNP concentration $\boldsymbol{C_1}^{*m,m}$ to the detector readings at time step $m = 4, 8, 12, 16, \text{and} \, 20$ (2, 4, 6, 8, and 10 s into the transient) are plotted in Fig. 6. It is shown that $\phi_1^{*m,m} < \phi_2^{*m,m}$ despite $\Sigma_{d,1} > \Sigma_{d,2}$, which suggests that Σ_d is not the only factor that impacted the importance of the particles. It is also shown that $\phi_1^{*m,m}$ and $\phi_2^{*m,m}$ had the largest magnitude at 4 s, when the control rod was the most extracted, and had the smallest magnitude at 10 s, when the control rod was the most inserted. This suggests that the current-time adjoint fluxes are positively correlated to the neutron fluxes.

The time-dependent flux-normalized current-time adjoint fluxes are plotted in Fig. 7 together with the relative differences with respect to that at 4 s (with the largest flux). The nonzero differences suggest that the current-time adjoint fluxes are not proportional to the neutron fluxes. A maximum error of around 30% would be introduced if the current-time adjoint fluxes are calculated at only one specific moment in time and extended to other moments in time by weighting on the neutron fluxes. Solving the time-dependent adjoint systems is therefore necessary if good accuracy in the adjoint fluxes is required.

It is pointed out that we calculated only the adjoint solutions for the transient ($m \in [1, M]$) in this section because the adjoint solutions associated with the detector response did not exist for the specific steady state considered in this study, namely, the self-sustaining critical steady state. The adjoint equations of the steady state in this study can be written as

$$\boldsymbol{L}^*\phi^* = \boldsymbol{S}^*, \tag{37}$$

where $\boldsymbol{L}^* = \boldsymbol{L}^T$ as shown in Ref. 31 and $\boldsymbol{S}^*$ is the adjoint source depending on the characteristics and the location of the detector. $\boldsymbol{L}^*$ is noninvertible because $\boldsymbol{L}$ is noninvertible, as demonstrated in Sec. II.B. Therefore, Eq. (37) has no solutions unless $\boldsymbol{S}^*$ lies in the image of $\boldsymbol{L}^*$ (i.e., the span of vectors of the linear operator $\boldsymbol{L}^*$). However, $\boldsymbol{S}^*$ is uncontrolled as the characteristics and the location of the detector are not imposed.

Although the adjoint solutions of interest do not exist for the self-sustaining critical steady state, they exist for other types of steady state. For example, Cacuci[17] derived the analytical expression of the adjoint solutions associated with certain responses for steady states with external neutron sources. This is because when disturbances are introduced,

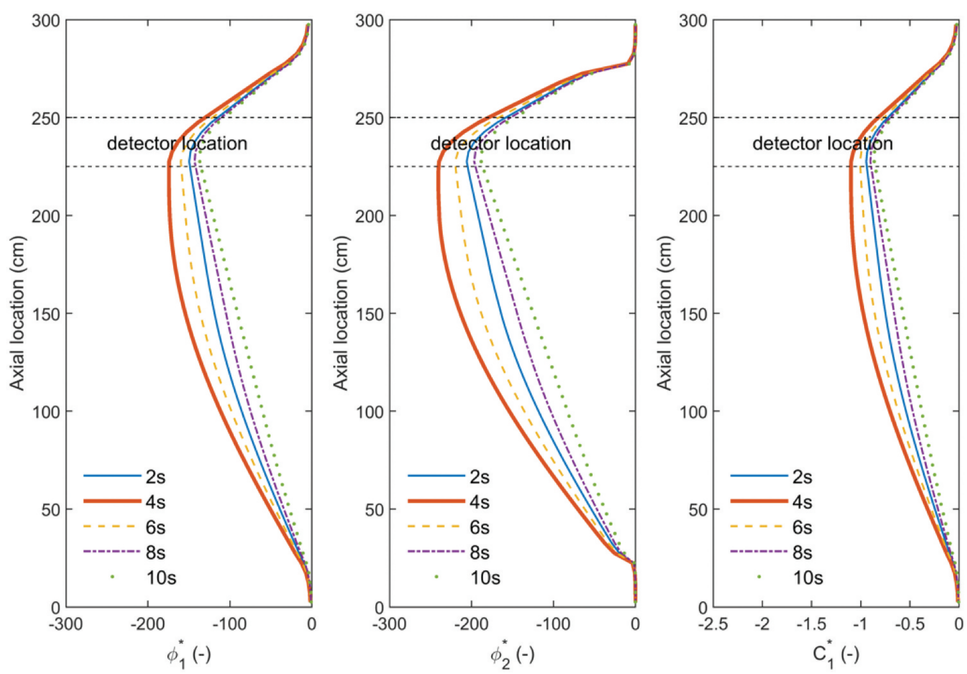

Fig. 6. Current-time continuous adjoint solutions to the detector readings at 2, 4, 6, 8, and 10 s.

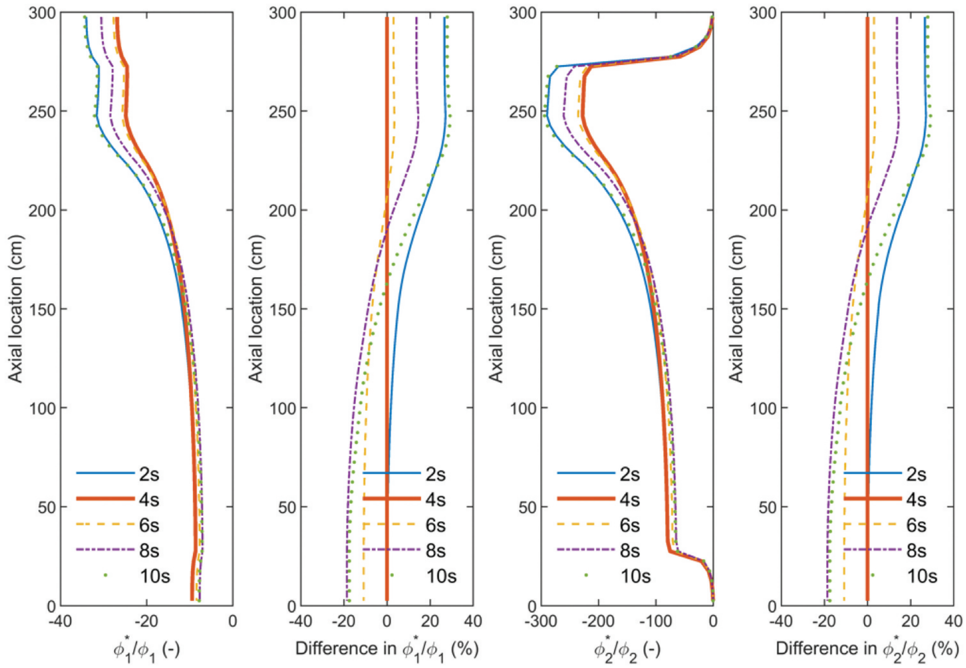

Fig. 7. Flux-normalized current-time continuous adjoint solutions to the detector readings at 2, 4, 6, 8, and 10s and the relative differences with respect to that at 4 s.

a new steady state with an external neutron source will be established while a self-sustaining critical state will not exist anymore.

IV. ADJOINT TRANSIENT CALCULATIONS WITH THE DISCRETE ADJOINT METHOD

The adjoint fluxes to the detector during the postulated REA in the simplified 1-D reactor are calculated by using the discrete adjoint method in this section to verify the results obtained in Sec. III.

IV.A. Discrete Adjoint Method

The discrete adjoint method calculates the adjoint solutions in a system through the following equation[7]:

$$\left(\frac{\partial \mathbb{N}}{\partial \phi}\right)^{T} \phi^{*} = -\left(\frac{\partial J}{\partial \phi}\right)^{T}, \tag{38}$$

where $\mathbb{N}$ represents the residual equations of the system, the components of which are actually given in Eqs. (6) through (13), and J represents a general response. Because the derivation of Eq. (38) has been discussed in detail in numerous existing references[7,34,35] as well as in one of our previous works,[23] it is not repeated in this paper. The response derivative $\frac{\partial J}{\partial \phi}$ can be expressed in the vector form as

$$\left(\frac{\partial J}{\partial \phi}\right)^{T} = \left(\frac{\partial J}{\partial \phi_1^1} \quad \frac{\partial J}{\partial \phi_1^2} \quad \cdots \quad \frac{\partial J}{\partial C_6^{M-1}} \quad \frac{\partial J}{\partial C_6^{M-1}}\right)^{T}_{\in(8NM,1)}. \tag{39}$$

When the detector readings at time step m are of interest,

$$J^m = \sum_{j=11}^{15}\left(\Sigma_{d,1}\phi_{1,j}^m + \Sigma_{d,2}\phi_{2,j}^m\right) \tag{40}$$

and

$$\left(\frac{\partial J^m}{\partial \phi}\right)^{T}(8N(m-1)+j) = \begin{cases} \Sigma_{d,1} \text{ if } (i = m \text{ and } j \in [p(I_d-1)+1, pI_d]) \\ \Sigma_{d,2} \text{if } (i = m \text{ and } j \in [p(I_d-1)+1+N, pI_d+N]), \\ 0 \text{ if else} \end{cases} \tag{41}$$

with p, I_d, and N similar to those in Eq. (36). Considering the simplified 1-D reactor in this study, the derivative to the residual function $\frac{\partial \mathbb{N}}{\partial \phi}$ can be expressed in matrix form as

$$\frac{\partial \mathbb{N}}{\partial \phi} = \begin{pmatrix} \frac{\partial \mathbb{N}^1}{\partial \phi^1} & \frac{\partial \mathbb{N}^1}{\partial \phi^2} & \cdots & \frac{\partial \mathbb{N}^1}{\partial \phi^{M-1}} & \frac{\partial \mathbb{N}^1}{\partial \phi^M} \\ \frac{\partial \mathbb{N}^2}{\partial \phi^1} & \frac{\partial \mathbb{N}^2}{\partial \phi^2} & \cdots & \frac{\partial \mathbb{N}^2}{\partial \phi^{M-1}} & \frac{\partial \mathbb{N}^2}{\partial \phi^M} \\ \vdots & \vdots & & \vdots & \vdots \\ \frac{\partial \mathbb{N}^{M-1}}{\partial \phi^1} & \frac{\partial \mathbb{N}^{M-1}}{\partial \phi^2} & \cdots & \frac{\partial \mathbb{N}^{M-1}}{\partial \phi^{M-1}} & \frac{\partial \mathbb{N}^{M-1}}{\partial \phi^M} \\ \frac{\partial \mathbb{N}^M}{\partial \phi^1} & \frac{\partial \mathbb{N}^M}{\partial \phi^2} & \cdots & \frac{\partial \mathbb{N}^M}{\partial \phi^{M-1}} & \frac{\partial \mathbb{N}^M}{\partial \phi^M} \end{pmatrix}_{\in(8NM,8NM)} , \tag{42}$$

where

$$\frac{\partial \mathbb{N}^m}{\partial \phi^i} = \begin{pmatrix} \frac{\partial \mathbb{N}^m_{1,1}}{\partial \phi^i_{1,1}} & \frac{\partial \mathbb{N}^m_{1,1}}{\partial \phi^i_{1,2}} & \cdots & \frac{\partial \mathbb{N}^m_{1,1}}{\partial C^i_{6,N-1}} & \frac{\partial \mathbb{N}^m_{1,1}}{\partial C^i_{6,N}} \\ \frac{\partial \mathbb{N}^m_{1,2}}{\partial \phi^i_{1,1}} & \frac{\partial \mathbb{N}^m_{1,2}}{\partial \phi^i_{1,2}} & \cdots & \frac{\partial \mathbb{N}^m_{1,2}}{\partial C^i_{6,N-1}} & \frac{\partial \mathbb{N}^m_{1,2}}{\partial C^i_{6,N}} \\ \vdots & \vdots & & \vdots & \vdots \\ \frac{\partial \mathbb{N}^m_{8,N-1}}{\partial \phi^i_{1,1}} & \frac{\partial \mathbb{N}^m_{8,N-1}}{\partial \phi^i_{1,2}} & \cdots & \frac{\partial \mathbb{N}^m_{8,N-1}}{\partial C^i_{6,N-1}} & \frac{\partial \mathbb{N}^m_{8,N-1}}{\partial C^i_{6,N}} \\ \frac{\partial \mathbb{N}^m_{8,N}}{\partial \phi^i_{1,1}} & \frac{\partial \mathbb{N}^m_{8,N}}{\partial \phi^i_{1,1}} & \cdots & \frac{\partial \mathbb{N}^m_{8,N}}{\partial C^i_{6,N-1}} & \frac{\partial \mathbb{N}^m_{8,N}}{\partial C^i_{6,N}} \end{pmatrix}_{\in(8N,8N)} (m, i \in [1, M]) . \tag{43}$$

By plugging in the expressions of the residual equations shown in Eqs. (6) through (13), we observe that

$$\frac{\partial \mathbb{N}^m}{\partial \phi^i} = \begin{cases} \mathcal{M}^m & \text{if } (i = m) \\ \boldsymbol{K}^m & \text{if} (i = m-1) \\ 0 & \text{if else} \end{cases} . \tag{44}$$

Because the $\mathbb{N}$'s are linear to the variable ϕ's, the matrix $\left(\frac{\partial \mathbb{N}}{\partial \phi}\right)^{\boldsymbol{T}}$ can then be further simplified as

$$\left(\frac{\partial \mathbb{N}}{\partial \phi}\right)^{\boldsymbol{T}} = \begin{pmatrix} (\mathcal{M}^1)^{\boldsymbol{T}} & (\boldsymbol{K}^2)^{\boldsymbol{T}} & \mathbf{0} & \cdots & \cdots & \cdots & \mathbf{0} \\ \mathbf{0} & (\mathcal{M}^2)^{\boldsymbol{T}} & (\boldsymbol{K}^3)^{\boldsymbol{T}} & \mathbf{0} & \cdots & \cdots & \mathbf{0} \\ \mathbf{0} & \mathbf{0} & (\mathcal{M}^3)^{\boldsymbol{T}} & (\boldsymbol{K}^4)^{\boldsymbol{T}} & \mathbf{0} & \cdots & \mathbf{0} \\ \vdots & & \ddots & \ddots & \ddots & \ddots & \vdots \\ \mathbf{0} & \cdots & \cdots & \mathbf{0} & (\mathcal{M}^{M-2})^{\boldsymbol{T}} & (\boldsymbol{K}^{M-1})^{\boldsymbol{T}} & \mathbf{0} \\ \mathbf{0} & \cdots & \cdots & \cdots & \mathbf{0} & (\mathcal{M}^{M-1})^{\boldsymbol{T}} & (\boldsymbol{K}^M)^{\boldsymbol{T}} \\ \mathbf{0} & \cdots & \cdots & \cdots & \cdots & \mathbf{0} & (\mathcal{M}^M)^{\boldsymbol{T}} \end{pmatrix}_{\in(8NM,8NM)} , \tag{45}$$

with $\left(\frac{\partial \mathbb{N}}{\partial \phi}\right)^{\boldsymbol{T}}$ and $\left(\frac{\partial J}{\partial \phi}\right)^{\boldsymbol{T}}$ straightened, and we then can obtain the time-dependent adjoint solutions by varying m from M to 1 and recurrently solving Eq. (38). It can be seen that since the discrete adjoint method worked directly on the discretized form of the forward equations, the consistent boundary conditions of the adjoint equations were naturally counted by the realization of Eq. (38) with no additional considerations. On the other hand, the final state condition should still be implicitly specified in a consistent manner in the discrete adjoint method because Eq. (38) has to be solved in the backward direction as well. In addition, since the adjoint discrete method precludes the need of deriving the continuous adjoint equations (in some cases, the derivation procedure could be prohibitive), it makes the method more straightforward to implement. All these desirable features can be considered as advantages of the discrete adjoint method whereas straightening the needed matrices in the discrete adjoint method as shown above takes some effort.

IV.B. Transient Adjoint Solutions by the Discrete Adjoint Method

Similar to the results by the continuous adjoint method, the time-dependent discrete adjoint solutions of the fast group neutron flux $\phi_1^{*m,i}$, the thermal group neutron flux $\phi_2^{*m,i}$, and the first-family DNP concentration $\boldsymbol{C}_1^{*m,i}$ to the detector readings at time step $m = 10$ (5 s into the transient) are plotted in Fig. 8.

Figure 8 resembles Fig. 5, while more thorough numerical comparisons indicate that all the continuous adjoint solutions and all the discrete adjoint solutions had exactly the same values in this study, which verifies the continuous adjoint solutions calculated in Sec. III.

By comparing Eq. (15) with Eq. (31), and Eq. (16) with Eq. (32) (detailed expressions of the coefficients are shown in Secs. A.II and A.IV, respectively), we can see that $(\mathcal{M}^{\boldsymbol{m}})^{\boldsymbol{T}}$ resembles $\mathcal{M}^{*\boldsymbol{m}}(m \in [1, M])$ and $(\boldsymbol{K}^{\boldsymbol{m}+1})^{\boldsymbol{T}}$ resembles $\boldsymbol{K}^{*\boldsymbol{m}}(m \in [1, M-1])$, except $\Delta t_{m-1\to m}$ (i.e., $t_m - t_{m-1}$) is employed in $(\mathcal{M}^{\boldsymbol{m}})^{\boldsymbol{T}}$ and $(\boldsymbol{K}^{\boldsymbol{m}+1})^{\boldsymbol{T}}$ while $\Delta t_{m\to m+1}$ (i.e., $t_{m+1} - t_m$) is employed in $\mathcal{M}^{*\boldsymbol{m}}$ and $\boldsymbol{K}^{*\boldsymbol{m}}$. When $\Delta t_{m-1\to m} = \Delta t_{m\to m+1}$, which is the case in this study as we used uniform time steps, $(\mathcal{M}^{\boldsymbol{m}})^{\boldsymbol{T}} = \mathcal{M}^{*\boldsymbol{m}}$ and $(\boldsymbol{K}^{\boldsymbol{m}+1})^{\boldsymbol{T}} = \boldsymbol{K}^{*\boldsymbol{m}}$. The left-hand side of Eq. (33) and that of Eq. (38) are therefore equivalent. Moreover, these two equations had the same right-hand side as $\boldsymbol{S}^{*\boldsymbol{m}} = \left(\frac{\partial J^m}{\partial \phi}\right)^{\boldsymbol{T}}$, which can be clearly seen by comparing Eq. (36) with Eq. (40). Therefore, the continuous adjoint solutions and the discrete adjoint solutions have the same values. In light of the discussions above, for multigroup neutron diffusion systems, calculating time-dependent adjoint solutions using either the continuous method or the discrete method is equivalent, considering both performance and computational expense. This finding agrees with statements existing in the literature that the continuous and the discrete adjoint methods have similar performance when they are applied to thermal-hydraulic problems.[7,23]

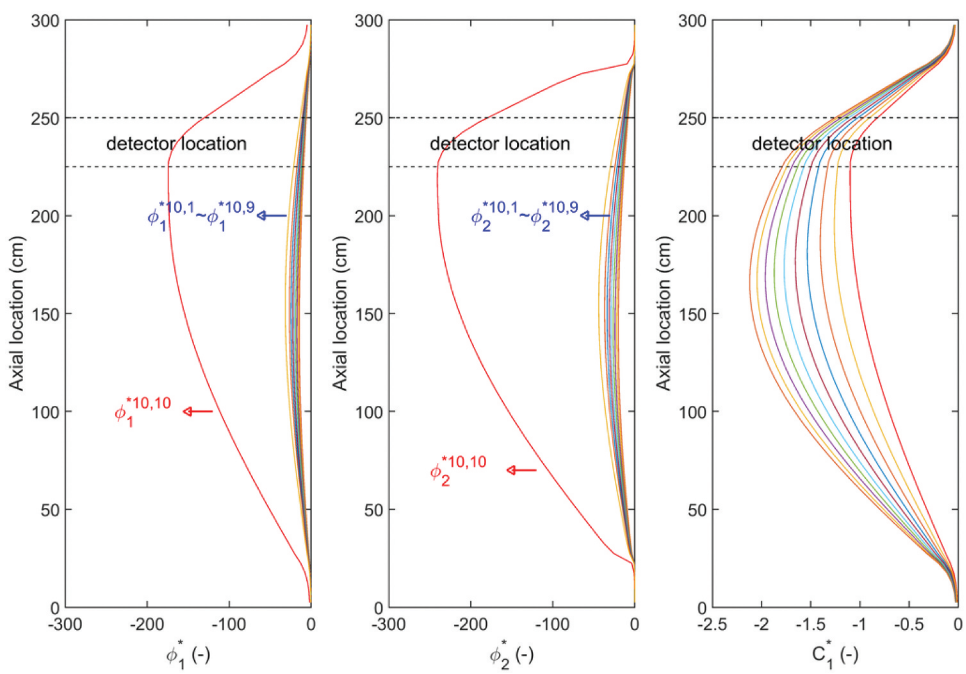

Fig. 8. Time-dependent discrete adjoint solutions to the detector readings at time step $m = 10$ (5 s into the transient).

ANS

It is pointed out that the adjoint fluxes may have opposite signs depending on the definition of the system under consideration. More specifically, the continuous adjoint fluxes would have opposite signs if a minus sign was added to both sides of the residual equations of the system $\mathbb{N}$ whose components are expressed in Eqs. (6) through (13). Similarly, the discrete adjoint fluxes would have opposite signs if a minus sign was added to both sides of Eq. (29) before considerating the adjoint source. However, the change in the sign of the adjoint fluxes does not have an impact on the physical sensitivities. By using the discrete sensitivity method,[23] the sensitivity of a general response $\boldsymbol{J}$ with respect to a system parameter $\boldsymbol{\theta}$ can be calculated as

$$\frac{\delta \boldsymbol{J}(\phi)}{\delta \boldsymbol{\theta}} = \phi^{*\boldsymbol{T}} \frac{\partial \mathbb{N}(\phi, \boldsymbol{\theta})}{\partial \boldsymbol{\theta}}. \tag{46}$$

When a minus sign is added to $\mathbb{N}$, both ϕ^* and $\frac{\partial \mathbb{N}(\phi,\boldsymbol{\theta})}{\partial \boldsymbol{\theta}}$ will have opposite signs while the sensitivity $\frac{\delta \boldsymbol{J}(\phi)}{\delta \boldsymbol{\theta}}$ remains unchanged.

V. SUMMARY AND CONCLUSIONS

The adjoint flux, which can be understood as the importance of particles, is a key concept in nuclear engineering because it is indispensable for the adjoint sensitivity analysis of some system parameters that are crucial for reactor safety. However, partly because of the excessive computational cost, adjoint fluxes are usually calculated only at steady states for eigenvalue problems and further used to estimate the time-dependent adjoint fluxes.

In this study, we demonstrated the necessity of calculating time-dependent adjoint fluxes by solving time-dependent adjoint systems rather than taking approximations from steady-state solutions. A postulated REA in a simplified 1-D nuclear reactor was considered as the case study. We calculated the adjoint fluxes of the two-group diffusion model of the case study by using the continuous adjoint method and identified the following two advantages:

1. *Unique feature*: The importance of particles at a certain moment in time to a specific response at another moment can be quantified by solving the time-dependent adjoint systems, which cannot be obtained from the steady-state adjoint solutions.

2. *Better accuracy*: Errors (around 30% maximum for the case study) would be introduced if the current-time adjoint fluxes are calculated at only one specific moment in time and extended to other moments in time by weighting on the time-dependent neutron fluxes.

Therefore, solving time-dependent adjoint systems is necessary if the unique feature described above is required or if a certain accuracy criterion needs to be met.

Meanwhile, we calculated the adjoint fluxes of the two-group diffusion model by using the alternative discrete adjoint method. The adjoint fluxes calculated by both the continuous and the discrete adjoint methods were the same, as demonstrated by the case study, which verified the correctness of each other. Moreover, the perfect agreement of the two results also proved the computational equivalence of the two adjoint methods when they were applied to the multigroup neutron diffusion problems. This finding agrees with the conclusion in the literature that the continuous and the discrete adjoint methods have similar performance when they are applied to thermal-hydraulic problems.[7]

Finally, the final state condition required by the backward type of adjoint diffusion equations, which had remained ambiguous in the literature, is clearly addressed in this paper, the meaning of which is explained with physics insights. The clarified final condition was applied in the case study, and the accuracy of the adjoint solutions in the application further justifies the correct definition and implementation of the final condition for adjoint systems.

APPENDIX

A.I. COEFFICIENTS IN (6) THROUGH EQS. (13)

The coefficients occurring in Eqs. (6) through (13) in Sec. II.C are expressed in Eqs. (A.1) through (A.40) as follows. Note that $\Delta x_{n-1/2}$ is calculated as the arithmetic mean of the adjacent meshes as $\Delta x_{n-1/2} = (\Delta x_n + \Delta x_{n-1})/2$, and $D_{n-1/2}$ is calculated as the harmonic mean of that in the adjacent meshes as $D_{n-1/2} = \frac{2}{\frac{1}{D_n} + \frac{1}{D_{n-1}}}$:

$$A^m_{1,n,n-1} = \begin{cases} 0 & \text{if}(n = 1) \\ -\dfrac{D^m_{1,n-1/2}}{\Delta x_n \Delta x_{n-1/2}} & \text{if}(1 < n \le N) \end{cases}, \tag{A.1}$$

$$A^m_{(1,n,n)} = \begin{cases} \frac{1}{v_1 \Delta t_{m-1\to m}} + \frac{D^m_{1,n+1/2}}{\Delta x_n \Delta x_{n+1/2}} + \Sigma^m_{r,1,n} - (1-\beta_{tot})\nu\Sigma^m_{f,1,n} & \text{if } (n=1) \\ \frac{1}{v_1 \Delta t_{m-1\to m}} + \frac{D^m_{1,n-1/2}}{\Delta x_n \Delta x_{n-1/2}} + \frac{D^m_{1,n+1/2}}{\Delta x_n \Delta x_{n+1/2}} + \Sigma^m_{r,1,n} - (1-\beta_{tot})\nu\Sigma^m_{f,1,n} & \text{if } (1 < n < N) \\ \frac{1}{v_1 \Delta t_{m-1\to m}} + \frac{D^m_{1,n-1/2}}{\Delta x_n \Delta x_{n-1/2}} + \Sigma^m_{r,1,n} - (1-\beta_{tot})\nu\Sigma^m_{f,1,n} & \text{if } (n=N)\,, \end{cases} \tag{A.2}$$

$$A^m_{1,n,n+1} = \begin{cases} -\frac{D_{1,n+1/2}}{\Delta x_n \Delta x_{n+1/2}} & \text{if } (1 \le n < N) \\ 0 & \text{if } (n = N) \end{cases}\,, \tag{A.3}$$

$$B^m_{1,n,n} = -(1-\beta_{tot})\nu\Sigma^m_{f,2,n}\,, \tag{A.4}$$

$$D^m_{1,n,n} = -\lambda_1\,, \tag{A.5}$$

$$E^m_{1,n,n} = -\lambda_2\,, \tag{A.6}$$

$$F^m_{1,n,n} = -\lambda_3\,, \tag{A.7}$$

$$G^m_{1,n,n} = -\lambda_4\,, \tag{A.8}$$

$$H^m_{1,n,n} = -\lambda_5\,, \tag{A.9}$$

$$L^m_{1,n,n} = -\lambda_6\,, \tag{A.10}$$

$$K^m_{1,n,n} = -\frac{1}{v_1 \Delta t_{m-1\to m}}\,, \tag{A.11}$$

$$A^m_{2,n,n} = -\Sigma^m_{s,1\to 2,n}\,, \tag{A.12}$$

$$B^m_{2,n,n-1} = \begin{cases} 0 & \text{if}(n=1) \\ -\frac{D^m_{2,n-1/2}}{\Delta x_n \Delta x_{n-1/2}} & \text{if}(1 < n \le N) \end{cases}\,, \tag{A.13}$$

$$B^m_{(2,n,n)} = \begin{cases} \frac{1}{v_2 \Delta t_{m-1\to m}} + \frac{D^m_{2,n+1/2}}{\Delta x_n \Delta x_{n+1/2}} + \Sigma^m_{a,2,n} & \text{if}(n=1) \\ \frac{1}{v_2 \Delta t_{m-1\to m}} + \frac{D^m_{2,n-1/2}}{\Delta x_n \Delta x_{n-1/2}} + \frac{D^m_{1,n+1/2}}{\Delta x_n \Delta x_{n+1/2}} + \Sigma^m_{a,2,n} & \text{if}(1 < n < N) \\ \frac{1}{v_2 \Delta t_{m-1\to m}} + \frac{D^m_{2,n-1/2}}{\Delta x_n \Delta x_{n-1/2}} + \Sigma^m_{a,2,n} & \text{if}(n = \mathrm{N})\,, \end{cases} \tag{A.14}$$

$$B^m_{2,n,n+1} = \begin{cases} -\frac{D_{2,n+1/2}}{\Delta x_n \Delta x_{n+1/2}} & \text{if } (1 \le n < N) \\ 0 & \text{if } (n = N) \end{cases}\,, \tag{A.15}$$

$$K_{2,n,n}^{m} = -\frac{1}{v_1 \Delta t_{m-1\to m}} , \tag{A.16}$$

$$A_{3,n,n}^{m} = -\beta_1 \nu \Sigma_{f,1,n}^{m} , \tag{A.17}$$

$$B_{3,n,n}^{m} = -\beta_1 \nu \Sigma_{f,2,n}^{m} , \tag{A.18}$$

$$D_{3,n,n}^{m} = \frac{1}{\Delta t_{m-1\to m}} + \lambda_1 , \tag{A.19}$$

$$K_{3,n,n}^{m} = -\frac{1}{\Delta t_{m-1\to m}} , \tag{A.20}$$

$$A_{4,n,n}^{m} = -\beta_2 \nu \Sigma_{f,1,n}^{m} , \tag{A.21}$$

$$B_{4,n,n}^{m} = -\beta_2 \nu \Sigma_{f,2,n}^{m} , \tag{A.22}$$

$$E_{4,n,n}^{m} = \frac{1}{\Delta t_{m-1\to m}} + \lambda_2 , \tag{A.23}$$

$$K_{4,n,n}^{m} = -\frac{1}{\Delta t_{m-1\to m}} , \tag{A.24}$$

$$A_{5,n,n}^{m} = -\beta_3 \nu \Sigma_{f,1,n}^{m} , \tag{A.25}$$

$$B_{5,n,n}^{m} = -\beta_3 \nu \Sigma_{f,2,n}^{m} , \tag{A.26}$$

$$F_{5,n,n}^{m} = \frac{1}{\Delta t_{m-1\to m}} + \lambda_3 , \tag{A.27}$$

$$K_{5,n,n}^{m} = -\frac{1}{\Delta t_{m-1\to m}} , \tag{A.28}$$

$$A_{6,n,n}^{m} = -\beta_4 \nu \Sigma_{f,1,n}^{m} , \tag{A.29}$$

$$B_{6,n,n}^{m} = -\beta_4 \nu \Sigma_{f,2,n}^{m} , \tag{A.30}$$

$$G_{6,n,n}^{m} = \frac{1}{\Delta t_{m-1\to m}} + \lambda_4 , \tag{A.31}$$

$$K_{6,n,n}^{m} = -\frac{1}{\Delta t_{m-1\to m}} , \tag{A.32}$$

$$A_{7,n,n}^{m} = -\beta_5 \nu \Sigma_{f,1,n}^{m} , \tag{A.33}$$

$$B_{7,n,n}^{m} = -\beta_5 \nu \Sigma_{f,2,n}^{m} , \tag{A.34}$$

$$H_{7,n,n}^{m} = \frac{1}{\Delta t_{m-1\to m}} + \lambda_5 , \tag{A.35}$$

$$K_{7,n,n}^{m} = -\frac{1}{\Delta t_{m-1\to m}} , \tag{A.36}$$

$$A_{8,n,n}^{m} = -\beta_6 \nu \Sigma_{f,1,n}^{m} , \tag{A.37}$$

$$B_{8,n,n}^{m} = -\beta_6 \nu \Sigma_{f,2,n}^{m} , \tag{A.38}$$

$$L_{8,n,n}^{m} = \frac{1}{\Delta t_{m-1\to m}} + \lambda_6 , \tag{A.39}$$

and

$$K_{8,n,n}^{m} = -\frac{1}{\Delta t_{m-1\to m}} . \tag{A.40}$$

A.II. SUBMATRICES IN EQS. (15), (16), AND (17)

The submatrices occurring in Eqs. (15), (16), and (17) in Sec. II.C are expressed in Eqs. (A.41) through (A.59) as follows:

$$\boldsymbol{A_1^m} = \begin{pmatrix} A^m_{1,1,1} & A^m_{1,1,2} & 0 & \cdots & \cdots & \cdots & 0 \\ A^m_{1,2,1} & A^m_{1,2,2} & A^m_{1,2,3} & 0 & & & \vdots \\ 0 & A^m_{1,3,2} & A^m_{1,3,3} & A^m_{1,3,4} & \ddots & & \vdots \\ \vdots & 0 & \ddots & \ddots & \ddots & 0 & \vdots \\ \vdots & & \ddots & A^m_{1,N-2,N-3} & A^m_{1,N-2,N-2} & A^m_{1,N-2,N-1} & 0 \\ \vdots & & & 0 & A^m_{1,N-1,N-2} & A^m_{1,N-1,N-1} & A^m_{1,N-1,N} \\ 0 & \cdots & \cdots & \cdots & 0 & A^m_{1,N,N-1} & A^m_{1,N,N} \end{pmatrix}_{\in(N,N)} , \tag{A.41}$$

$$\boldsymbol{A_i^m} = \begin{pmatrix} A^m_{i,1,1} & 0 & \cdots & \cdots & 0 \\ 0 & A^m_{i,2,2} & 0 & & \vdots \\ \vdots & \ddots & \ddots & \ddots & \vdots \\ \vdots & & \ddots & \ddots & 0 \\ 0 & \cdots & \cdots & 0 & A^m_{i,N,N} \end{pmatrix}_{\in(N,N)} \quad \text{if } i = 2 \text{ to } 8 , \tag{A.42}$$

$$\boldsymbol{B_i^m} = \begin{pmatrix} B^m_{i,1,1} & 0 & \cdots & \cdots & 0 \\ 0 & B^m_{i,2,2} & 0 & & \vdots \\ \vdots & \ddots & \ddots & \ddots & \vdots \\ \vdots & & \ddots & \ddots & 0 \\ 0 & \cdots & \cdots & 0 & B^m_{i,N,N} \end{pmatrix}_{\in(N,N)} \quad \text{if } i = 1 \text{ or } 3 \text{ to } 8 , \tag{A.43}$$

$$\boldsymbol{B_2^m} = \begin{pmatrix} B^m_{2,1,1} & B^m_{2,1,2} & 0 & \cdots & \cdots & \cdots & 0 \\ B^m_{2,2,1} & B^m_{2,2,2} & B^m_{2,2,3} & 0 & & & \vdots \\ 0 & B^m_{2,3,2} & B^m_{2,3,3} & B^m_{2,3,4} & \ddots & & \vdots \\ \vdots & \ddots & \ddots & \ddots & \ddots & \ddots & \vdots \\ \vdots & & \ddots & B^m_{2,N-2,N-3} & B^m_{2,N-2,N-2} & B^m_{2,N-2,N-1} & 0 \\ \vdots & & & 0 & B^m_{2,N-1,N-2} & B^m_{2,N-1,N-1} & B^m_{2,N-1,N} \\ 0 & \cdots & \cdots & \cdots & 0 & B^m_{2,N,N-1} & B^m_{2,N,N} \end{pmatrix}_{\in(N,N)} , \tag{A.44}$$

$$\boldsymbol{D_i^m} = \begin{pmatrix} D^m_{i,1,1} & 0 & \cdots & \cdots & 0 \\ 0 & D^m_{i,2,2} & 0 & & \vdots \\ \vdots & \ddots & \ddots & \ddots & \vdots \\ \vdots & & \ddots & \ddots & 0 \\ 0 & \cdots & \cdots & 0 & D^m_{i,N,N} \end{pmatrix}_{\in(N,N)} \quad \text{if } i = 1 \text{ or } 3 , \tag{A.45}$$

$$\boldsymbol{E_i^m} = \begin{pmatrix} E_{i,1,1}^m & 0 & \cdots & \cdots & 0 \\ 0 & E_{i,2,2}^m & 0 & & \vdots \\ \vdots & \ddots & \ddots & \ddots & \vdots \\ \vdots & & \ddots & \ddots & 0 \\ 0 & \cdots & \cdots & 0 & E_{i,N,N}^m \end{pmatrix}_{\in(\boldsymbol{N},\boldsymbol{N})} \quad \text{if } i = 1 \text{ or } 4\,, \tag{A.46}$$

$$\boldsymbol{F_i^m} = \begin{pmatrix} F_{i,1,1}^m & 0 & \cdots & \cdots & 0 \\ 0 & F_{i,2,2}^m & 0 & & \vdots \\ \vdots & \ddots & \ddots & \ddots & \vdots \\ \vdots & & \ddots & \ddots & 0 \\ 0 & \cdots & \cdots & 0 & F_{i,N,N}^m \end{pmatrix}_{\in(N,N)} \quad \text{if } i = 1 \text{ or } 5\,, \tag{A.47}$$

$$\boldsymbol{G_i^m} = \begin{pmatrix} G_{i,1,1}^m & 0 & \cdots & \cdots & 0 \\ 0 & G_{i,2,2}^m & 0 & & \vdots \\ \vdots & \ddots & \ddots & \ddots & \vdots \\ \vdots & & \ddots & \ddots & 0 \\ 0 & \cdots & \cdots & 0 & G_{i,N,N}^m \end{pmatrix}_{\in(N,N)} \quad \text{if } i = 1 \text{ or } 6\,, \tag{A.48}$$

$$\boldsymbol{H_i^m} = \begin{pmatrix} H_{i,1,1}^m & 0 & \cdots & \cdots & 0 \\ 0 & H_{i,2,2}^m & 0 & & \vdots \\ \vdots & \ddots & \ddots & \ddots & \vdots \\ \vdots & & \ddots & \ddots & 0 \\ 0 & \cdots & \cdots & 0 & H_{i,N,N}^m \end{pmatrix}_{\in(N,N)} \quad \text{if } i = 1 \text{ or } 7\,, \tag{A.49}$$

$$\boldsymbol{L_i^m} = \begin{pmatrix} L_{i,1,1}^m & 0 & \cdots & \cdots & 0 \\ 0 & L_{i,2,2}^m & 0 & & \vdots \\ \vdots & \ddots & \ddots & \ddots & \vdots \\ \vdots & & \ddots & \ddots & 0 \\ 0 & \cdots & \cdots & 0 & L_{i,N,N}^m \end{pmatrix}_{\in(N,N)} \quad \text{if } i = 1 \text{ or } 8\ \,, \tag{A.50}$$

$$\boldsymbol{K_i^m} = -\begin{pmatrix} K_{i,1,1}^m & 0 & \cdots & \cdots & 0 \\ 0 & K_{i,2,2}^m & 0 & & \vdots \\ \vdots & \ddots & \ddots & \ddots & \vdots \\ \vdots & & \ddots & \ddots & 0 \\ 0 & \cdots & \cdots & 0 & K_{i,N,N}^m \end{pmatrix}_{\in(N,N)} \quad \text{if } i = 1 \text{ to } 8\,, \tag{A.51}$$

$$\boldsymbol{\phi_1^m} = \begin{pmatrix} \phi_{1,1}^m & \cdots & \phi_{1,N}^m \end{pmatrix}^T_{\in(N,1)}\,, \tag{A.52}$$

$$\boldsymbol{\phi_2^m} = \begin{pmatrix} \phi_{2,1}^m & \cdots & \phi_{2,N}^m \end{pmatrix}^T_{\in(N,1)}\,, \tag{A.53}$$

$$\boldsymbol{C_1^m} = \begin{pmatrix} C_{1,1}^m & \cdots & C_{1,N}^m \end{pmatrix}^T_{\in(N,1)}\,, \tag{A.54}$$

$$\boldsymbol{C_2^m} = \begin{pmatrix} C_{2,1}^m & \cdots & C_{2,N}^m \end{pmatrix}^T_{\in(N,1)}\,, \tag{A.55}$$

$$\boldsymbol{C_3^m} = \left(C_{3,1}^m \quad \cdots \quad C_{3,N}^m \right)^T_{\in(N,1)} , \tag{A.56}$$

$$\boldsymbol{C_4^m} = \left(C_{4,1}^m \quad \cdots \quad C_{4,N}^m \right)^T_{\in(N,1)} , \tag{A.57}$$

$$\boldsymbol{C_5^m} = \left(C_{5,1}^m \quad \cdots \quad C_{5,N}^m \right)^T_{\in(N,1)} , \tag{A.58}$$

and

$$\boldsymbol{C_6^m} = \left(C_{6,1}^m \quad \cdots \quad C_{6,N}^m \right)^T_{\in(N,1)} . \tag{A.59}$$

A.III. COEFFICIENTS IN EQS. (21) THROUGH (28)

The coefficients occurring in Eqs. (21) through (28) in Sec. III.A are expressed in Eqs. (A.60) through (A.99) as follows:

$$A^{*m}_{1,n,n-1} = \begin{cases} 0 & \text{if}(n=1) \\ -\dfrac{D^m_{1,n-1/2}}{\Delta x_n \Delta x_{n-1/2}} & \text{if}(1 < n \le N) \end{cases} , \tag{A.60}$$

$$A^{*m}_{(1,n,n)} = \begin{cases} \dfrac{1}{v_1 \Delta t_{m\to m+1}} + \dfrac{D^m_{1,n+1/2}}{\Delta x_n \Delta x_{n+1/2}} + \Sigma^m_{r,1,n} - (1-\beta_{tot})\nu\Sigma^m_{f,1,n} & \text{if}(n=1) \\ \dfrac{1}{v_1 \Delta t_{m\to m+1}} + \dfrac{D^m_{1,n-1/2}}{\Delta x_n \Delta x_{n-1/2}} + \dfrac{D^m_{1,n+1/2}}{\Delta x_n \Delta x_{n+1/2}} + \Sigma^m_{r,1,n} - (1-\beta_{tot})\nu\Sigma^m_{f,1,n} & \text{if}(1 < n < N) \\ \dfrac{1}{v_1 \Delta t_{m\to m+1}} + \dfrac{D^m_{1,n-1/2}}{\Delta x_n \Delta x_{n-1/2}} + \Sigma^m_{r,1,n} - (1-\beta_{tot})\nu\Sigma^m_{f,1,n} & \text{if}(n=N) \end{cases} , \tag{A.61}$$

$$A^{*m}_{1,n+1} = \begin{cases} -\dfrac{D_{1,n+1/2}}{\Delta x_n \Delta x_{n+1/2}} & \text{if}(1 \le n < N) \\ 0 & \text{if}(n=N) \end{cases} , \tag{A.62}$$

$$B^{*m}_{1,n,n} = -\Sigma^m_{s,1\to 2,n} , \tag{A.63}$$

$$D^{*m}_{1,n,n} = -\beta_1 \nu\Sigma^m_{f,1,n} , \tag{A.64}$$

$$E^{*m}_{1,n} = -\beta_2 \nu\Sigma^m_{f,1,n} , \tag{A.65}$$

$$F^{*m}_{1,n} = -\beta_3 \nu\Sigma^m_{f,1,n} , \tag{A.66}$$

$$G^{*m}_{1,n} = -\beta_4 \nu\Sigma^m_{f,1,n} , \tag{A.67}$$

$$H^{*m}_{1,n} = -\beta_5 \nu\Sigma^m_{f,1,n} , \tag{A.68}$$

$$L^{*m}_{1,n} = -\beta_6 \nu\Sigma^m_{f,1,n} , \tag{A.69}$$

$$K^{*m}_{1,n} = -\frac{1}{v_1 \Delta t_{m\to m+1}} , \tag{A.70}$$

$$A^{*m}_{2,n,n} = -(1-\beta_{tot})\nu\Sigma^m_{f,2,n} , \tag{A.71}$$

$$B^{*m}_{2,n,n-1} = \begin{cases} 0 & \text{if}(n=1) \\ -\dfrac{D^m_{2,n-1/2}}{\Delta x_n \Delta x_{n-1/2}} & \text{if}(1n \le N) \end{cases} , \tag{A.72}$$

$$B^{*m}_{(2,n,n)} = \begin{cases} \dfrac{1}{v_2 \Delta t_{m\to m+1}} + \dfrac{D^m_{2,n+1/2}}{\Delta x_n \Delta x_{n+1/2}} + \Sigma^m_{a,2,n} & \text{if}(n=1) \\ \dfrac{1}{v_2 \Delta t_{m\to m+1}} + \dfrac{D^m_{2,n-1/2}}{\Delta x_n \Delta x_{n-1/2}} + \dfrac{D^m_{1,n+1/2}}{\Delta x_n \Delta x_{n+1/2}} + \Sigma^m_{a,2,n} & \text{if}(1 < n < N) \\ \dfrac{1}{v_2 \Delta t_{m\to m+1}} + \dfrac{D^m_{2,n-1/2}}{\Delta x_n \Delta x_{n-1/2}} + \Sigma^m_{a,2,n} & \text{if}(n=N) \end{cases} , \tag{A.73}$$

$$B^{*m}_{2,n,n+1} = \begin{cases} -\dfrac{D_{2,n+1/2}}{\Delta x_n \Delta x_{n+1/2}} & \text{if}(1 \le n < N) \\ 0 & \text{if}(n=N) \end{cases} , \tag{A.74}$$

$$D^{*m}_{2,n,n} = -\beta_1 \nu \Sigma^m_{f,2,n} , \tag{A.75}$$

$$E^{*m}_{2,n,n} = -\beta_2 \nu \Sigma^m_{f,2,n} , \tag{A.76}$$

$$F^{*m}_{2,n,n} = -\beta_3 \nu \Sigma^m_{f,2,n} , \tag{A.77}$$

$$G^{*m}_{2,n,n} = -\beta_4 \nu \Sigma^m_{f,2,n} , \tag{A.78}$$

$$H^{*m}_{2,n,n} = -\beta_5 \nu \Sigma^m_{f,2,n} , \tag{A.79}$$

$$L^{*m}_{2,n,n} = -\beta_6 \nu \Sigma^m_{f,2,n} , \tag{A.80}$$

$$K^{*m}_{2,n,n} = -\frac{1}{v_2 \Delta t_{m\to m+1}} , \tag{A.81}$$

$$A^{*m}_{3,n,n} = -\lambda_1 , \tag{A.82}$$

$$D^{*m}_{3,n,n} = \frac{1}{\Delta t_{m\to m+1}} + \lambda_1 , \tag{A.83}$$

$$K^{*m}_{3,n,n} = -\frac{1}{\Delta t_{m\to m+1}} , \tag{A.84}$$

$$A^{*m}_{4,n,n} = -\lambda_2 , \tag{A.85}$$

$$E^{*m}_{4,n,n} = \frac{1}{\Delta t_{m\to m+1}} + \lambda_2 , \tag{A.86}$$

$$K^{*m}_{4,n,n} = -\frac{1}{\Delta t_{m\to m+1}} , \tag{A.87}$$

$$A^{*m}_{5,n,n} = -\lambda_3 , \tag{A.88}$$

$$F^{*m}_{5,n,n} = \frac{1}{\Delta t_{m\to m+1}} + \lambda_3 , \tag{A.89}$$

$$K^{*m}_{5,n,n} = -\frac{1}{\Delta t_{m\to m+1}} , \tag{A.90}$$

$$A^{*m}_{6,n,n} = -\lambda_4 , \tag{A.91}$$

$$G^{*m}_{6,n,n} = \frac{1}{\Delta t_{m\to m+1}} + \lambda_4 , \tag{A.92}$$

$$K^{*m}_{6,n,n} = -\frac{1}{\Delta t_{m\to m+1}} , \tag{A.93}$$

$$A^{*m}_{7,n,n} = -\lambda_5 , \tag{A.94}$$

$$H^{*m}_{7,n,n} = \frac{1}{\Delta t_{m\to m+1}} + \lambda_5 , \tag{A.95}$$

$$K^{*m}_{7,n,n} = -\frac{1}{\Delta t_{m\to m+1}} , \tag{A.96}$$

$$A^{*m}_{8,n,n} = -\lambda_6 , \tag{A.97}$$

$$L^{*m}_{8,n,n} = \frac{1}{\Delta t_{m\to m+1}} + \lambda_6 , \tag{A.98}$$

and

$$K^{*m}_{8,n,n} = -\frac{1}{\Delta t_{m\to m+1}} . \tag{A.99}$$

A.IV. SUBMATRICES IN EQS. (31) AND (32)

The submatrices occurring in Eqs. (31) and (32) in Sec. III.A are expressed in Eqs. (A.100) through (A.110) as follows:

$$\boldsymbol{A}^{*\boldsymbol{m}}_{\boldsymbol{1}} = \begin{pmatrix} A^{*m}_{1,1,1} & A^{*m}_{1,1,2} & 0 & \cdots & \cdots & \cdots & 0 \\ A^{*m}_{1,2,1} & A^{*m}_{1,2,2} & A^{*m}_{1,2,3} & 0 & & & \vdots \\ 0 & A^{*m}_{1,3,2} & A^{*m}_{1,3,3} & A^{*m}_{1,3,4} & & & \vdots \\ \vdots & \ddots & \ddots & \ddots & \ddots & 0 & \vdots \\ \vdots & & \ddots & A^{*m}_{1,N-2,N-3} & A^{*m}_{1,N-2,N-2} & A^{*m}_{1,N-2,N-1} & 0 \\ \vdots & & & 0 & A^{*m}_{1,N-1,N-2} & A^{*m}_{1,N-1,N-1} & A^{*m}_{1,N-1,N} \\ 0 & \cdots & \cdots & \cdots & 0 & A^{*m}_{1,N,N-1} & A^{*m}_{1,N,N} \end{pmatrix}_{\in(N,N)}, \tag{A.100}$$

$$\boldsymbol{A}^{*\boldsymbol{m}}_{\boldsymbol{i}} = \begin{pmatrix} A^{*m}_{i,1,1} & 0 & \cdots & \cdots & 0 \\ 0 & A^{*m}_{i,2,2} & 0 & & \vdots \\ \vdots & \ddots & \ddots & \ddots & \vdots \\ \vdots & & \ddots & \ddots & 0 \\ 0 & \cdots & \cdots & 0 & A^{*m}_{i,N,N} \end{pmatrix}_{\in(N,N)} \quad \text{if} \quad i = 2 \text{ to } 8, \tag{A.101}$$

$$\boldsymbol{B}^{*\boldsymbol{m}}_{1} = \begin{pmatrix} B^{*m}_{1,1,1} & 0 & \cdots & \cdots & 0 \\ 0 & B^{*m}_{1,2,2} & 0 & & \vdots \\ \vdots & \ddots & \ddots & \ddots & \vdots \\ \vdots & & \ddots & \ddots & 0 \\ 0 & \cdots & \cdots & 0 & B^{*m}_{1,N,N} \end{pmatrix}_{\in(N,N)}, \tag{A.102}$$

$$\boldsymbol{B}^{*\boldsymbol{m}}_{\boldsymbol{2}} = \begin{pmatrix} B^{*m}_{2,1,1} & B^{*m}_{2,1,2} & 0 & \cdots & \cdots & \cdots & 0 \\ B^{*m}_{2,2,1} & B^{*m}_{2,2,2} & B^{*m}_{2,2,3} & 0 & & & \vdots \\ 0 & B^{*m}_{2,3,2} & B^{*m}_{2,3,3} & B^{*m}_{2,3,4} & 0 & & \vdots \\ \vdots & \ddots & \ddots & \ddots & \ddots & \ddots & \vdots \\ \vdots & & 0 & B^{*m}_{2,N-2,N-3} & B^{*m}_{2,N-2,N-2} & B^{*m}_{2,N-2,N-1} & 0 \\ \vdots & & & 0 & B^{*m}_{2,N-1,N-2} & B^{*m}_{2,N-1,N-1} & B^{*m}_{2,N-1,N} \\ 0 & \cdots & \cdots & \cdots & 0 & B^{*m}_{2,N,N-1} & B^{*m}_{2,N,N} \end{pmatrix}_{\in(N,N)}, \tag{A.103}$$

$$\boldsymbol{D}^{*\boldsymbol{m}}_{\boldsymbol{i}} = \begin{pmatrix} D^{*m}_{i,1,1} & 0 & \cdots & \cdots & 0 \\ 0 & D^{*m}_{i,2,2} & 0 & & \vdots \\ \vdots & \ddots & \ddots & \ddots & \vdots \\ \vdots & & \ddots & \ddots & 0 \\ 0 & \cdots & \cdots & 0 & D^{*m}_{i,N,N} \end{pmatrix}_{\in(N,N)} \quad \textit{if } i = 1, 2, \text{or } 3\,, \tag{A.104}$$

$$\boldsymbol{E}^{*\boldsymbol{m}}_{\boldsymbol{i}} = \begin{pmatrix} E^{*m}_{i,1,1} & 0 & \cdots & \cdots & 0 \\ 0 & E^{*m}_{i,2,2} & 0 & & \vdots \\ \vdots & \ddots & \ddots & \ddots & \vdots \\ \vdots & & \ddots & \ddots & 0 \\ 0 & \cdots & \cdots & 0 & E^{*m}_{i,N,N} \end{pmatrix}_{\in(\boldsymbol{N},\boldsymbol{N})} \quad \text{if } i = 1,\ 2 \text{ or } 4\,, \tag{A.105}$$

$$\boldsymbol{F}^{*\boldsymbol{m}}_{\boldsymbol{i}} = \begin{pmatrix} F^{*m}_{i,1,1} & 0 & \cdots & \cdots & 0 \\ 0 & F^{*m}_{i,2,2} & 0 & & \vdots \\ \vdots & \ddots & \ddots & \ddots & \vdots \\ \vdots & & \ddots & \ddots & 0 \\ 0 & \cdots & \cdots & 0 & F^{*m}_{i,N,N} \end{pmatrix}_{\in(N,N)} \quad \text{if } i = 1,\ 2 \text{ or } 5\,, \tag{A.106}$$

$$\boldsymbol{G}^{*\boldsymbol{m}}_{\boldsymbol{i}} = \begin{pmatrix} G^{*m}_{i,1,1} & 0 & \cdots & \cdots & 0 \\ 0 & G^{*m}_{i,2,2} & 0 & & \vdots \\ \vdots & \ddots & \ddots & \ddots & \vdots \\ \vdots & & \ddots & \ddots & 0 \\ 0 & \cdots & \cdots & 0 & G^{*m}_{i,N,N} \end{pmatrix}_{\in(N,N)} \quad \text{if } i = 1,\ 2 \text{ or } 6\,, \tag{A.107}$$

$$\boldsymbol{H}^{*\boldsymbol{m}}_{\boldsymbol{i}} = \begin{pmatrix} H^{*m}_{i,1,1} & 0 & \cdots & \cdots & 0 \\ 0 & H^{*m}_{i,2,2} & 0 & & \vdots \\ \vdots & \ddots & \ddots & \ddots & \vdots \\ \vdots & & \ddots & \ddots & 0 \\ 0 & \cdots & \cdots & 0 & H^{*m}_{i,N,N} \end{pmatrix}_{\in(N,N)} \quad \text{if } i = 1,\ 2 \text{ or } 7\,, \tag{A.108}$$

$$\boldsymbol{L}^{*\boldsymbol{m}}_{\boldsymbol{i}} = \begin{pmatrix} L^{*m}_{i,1,1} & 0 & \cdots & \cdots & 0 \\ 0 & L^{*m}_{i,2,2} & 0 & & \vdots \\ \vdots & \ddots & \ddots & \ddots & \vdots \\ \vdots & & \ddots & \ddots & 0 \\ 0 & \cdots & \cdots & 0 & L^{*m}_{i,N,N} \end{pmatrix}_{\in(N,N)} \quad \text{if } i = 1,\ 2 \text{ or } 8\,, \tag{A.109}$$

and

$$\boldsymbol{K}_{\boldsymbol{i}}^{*\boldsymbol{m}} = -\begin{pmatrix} K_{i,1,1}^{*m} & 0 & \cdots & \cdots & 0 \\ 0 & K_{i,2,2}^{*m} & 0 & & \vdots \\ \vdots & \ddots & \ddots & \ddots & \vdots \\ \vdots & & \ddots & \ddots & 0 \\ 0 & \cdots & \cdots & 0 & K_{i,N,N}^{*m} \end{pmatrix}_{\in(N,N)} \quad \text{if } i = 1 \text{ to } 8. \tag{A.110}$$

Disclosure Statement

No potential conflict of interest was reported by the author(s).

ORCID

Zeyun Wu http://orcid.org/0000-0002-6114-0352
Cihang Lu http://orcid.org/0000-0002-6385-6338

References

1. W. M. STACEY, *Nuclear Reactor Physics*, 2nd ed., Wiley-VCH, Weinheim, Germany (2007).
2. P. J. TURINSKY et al., "NESTLE Few-Group Neutron Diffusion Equation Solver Utilizing the Nodal Expansion Method for Eigenvalue, Adjoint, Fixed-Source Steady-State and Transient Problems," EGG-NRE-11406, Idaho National Engineering Laboratory (1994).
3. Q. WANG, "Forward and Adjoint Sensitivity Computation of Chaotic Dynamical Systems," *J. Comput. Phys.*, **235**, 1 (2013); https://doi.org/10.1016/j.jcp.2012.09.007.
4. S. LI and L. PETZOLD, "Adjoint Sensitivity Analysis for Time-Dependent Partial Differential Equations with Adaptive Mesh Refinement," *J. Comput. Phys.*, **198**, 310 (2004); https://doi.org/10.1016/j.jcp.2003.01.001.
5. M. WILLIAMS, *Handbook of Nuclear Reactor Calculations—Perturbation Theory for Nuclear Reactor Analysis*, Vol. III, CRC Press (1986).
6. Z. WU et al., "GPT-Free Sensitivity Analysis for Monte Carlo Models," *Nucl. Technol.*, **205**, *7*, 912 (2019); https://doi.org/10.1080/00295450.2018.1556062.
7. G. HU and T. KOZLOWSKI, "Application of Discrete Adjoint Method to Sensitivity and Uncertainty Analysis in Steady-State Two-Phase Flow Simulations," *Ann. Nucl. Energy*, **126**, 122 (2019); https://doi.org/10.1016/j.anucene.2018.11.012.
8. J. LEWINS, *Importance, The Adjoint Function*, Pergamon Press (1965).
9. R. ERRICO, "What Is an Adjoint Model?" *Bull. Am. Meteorol. Soc.*, **78**, 2577 (1997); https://doi.org/10.1175/1520-0477(1997)078<2577:WIAAM>2.0.CO;2.
10. M. ROCKLIN and E. M. CONSTANTINESCU, "Adjoint Sensitivity Analysis for Wind Power Generation," Argonne National Laboratory (2009).
11. S. SON and J. I. LEE, "Application of Adjoint Sensitivity Analysis Method to Supercritical CO_2 Power Cycle Optimization," *Energy*, **147**, 1153 (2018); https://doi.org/10.1016/j.energy.2018.01.117.
12. S. K. NADARAJAH, "The Discrete Adjoint Approach to Aerodynamic Shape," PhD Dissertation, Stanford University (2003).
13. J. P. THOMAS and E. H. DOWELL, "Discrete Adjoint Approach for Nonlinear Unsteady Aeroelastic Design Optimization," *AIAA J.*, **57**, *10*, 4368 (2019); https://doi.org/10.2514/1.J057504.
14. D. G. CACUCI et al., "Sensitivity Theory for General Systems of Nonlinear Equations," *Nucl. Sci. Eng.*, **75**, 88 (1980); https://doi.org/10.13182/NSE75-88.
15. D. G. CACUCI, "Sensitivity Theory for Nonlinear Systems. I. Nonlinear Functional Analysis Approach," *J. Math. Phys.*, **22**, *12*, 2794 (1981); https://doi.org/10.1063/1.525186.
16. D. G. CACUCI, "Sensitivity Theory for Nonlinear Systems. II. Extensions to Additional Classes of Responses," *J. Math. Phys.*, **22**, *12*, 2803 (1981); https://doi.org/10.1063/1.524870.
17. D. G. CACUCI, *Sensitivity and Uncertainty Analysis*, Chapman & Hall/CRC Press, Washington, D.C. (2003).
18. D. G. CACUCI et al., "A Heat Conduction and Convection Analytical Benchmark for Adjoint Solution Verification of Computational Fluid Dynamics Codes Used in Reactor Design," *Nucl. Sci. Eng.*, **182**, 452 (2016); https://doi.org/10.13182/NSE15-69.
19. D. G. CACUCI and E. WACHOLDER, "Adjoint Sensitivity Analysis for Transient Two-Phase Flow,"

Nucl. Sci. Eng., **82**, 461 (1982); https://doi.org/10.13182/NSE82-A21460.

20. D. G. CACUCI and M. IONESCU-BUJOR, "Adjoint Sensitivity Analysis of the RELAP5/MOD3.2 Two-Fluid Thermal-Hydraulic Code System—I: Theory," *Nucl. Sci. Eng.*, **136**, 59 (2000); https://doi.org/10.13182/NSE136-59.

21. M. IONESCU-BUJOR and D. G. CACUCI, "Adjoint Sensitivity Analysis of the RELAP5/MOD3.2 Two-Fluid Thermal-Hydraulic Code System—II: Applications," *Nucl. Sci. Eng.*, **136**, 85 (2000); https://doi.org/10.13182/NSE136-85.

22. A. C. DUFFY, "An Introduction to Gradient Computation by the Discrete Adjoint Method," Florida State University (2009).

23. C. LU and Z. WU, "Sensitivity Analysis of the 1-D SFR Thermal Stratification Model via Discrete Adjoint Sensitivity Method," *Nucl. Eng. Des.*, **370**, 110920 (2020); https://doi.org/10.1016/j.nucengdes.2020.110920.

24. A. GANDINI, "A Generalized Perturbation Method for Bi-Linear Functionals of the Real and Adjoint Neutron Fluxes," *J. Nucl. Eng.*, **21**, 755 (1967); https://doi.org/10.1016/0022-3107(67)90086-X.

25. L. L. SHERMAN et al., "First and Second-Order Aerodynamic Sensitivity Derivatives via Automatic Differentiation with Iterative Methods," *J. Comput. Phys.*, **129**, *2*, 307 (1996); https://doi.org/10.1006/jcph.1996.0252.

26. A. C. TAYLOR III and M. M. PUTKO, "Some Advanced Concepts in Discrete Aerodynamic Sensitivity Analysis," *AIAA J.*, **41**, *7*, 1224 (2003); https://doi.org/10.2514/2.2085.

27. B. G. VAN BLOEMEN WAANDERS et al., "Sensitivity Technologies for Large Scale Simulation," SAND2004-6574, Sandia National Laboratories (2005).

28. T. DOWNAR, Y. XU, and V. SEKER, "PARCS v3.0 U.S. NRC Core Neutronics Simulator Theory Manual," University of Michigan, Department of Nuclear Engineering and Radiological Sciences (2009).

29. Y. WANG, S. SCHUNERT, and V. LABOURE, "Rattlesnake Theory Manual," INL/EXT-17-42103, Idaho National Laboratory (2018).

30. G. I. BELL and S. GLASSTONE, *Nuclear Reactor Theory*, Van Nostrand Reinhold, New York (1970).

31. A. VIDAL-FERRÀNDIZ et al., "Moving Meshes to Solve the Time-Dependent Neutron Diffusion Equation in Hexagonal Geometry," *J. Comput. Appl. Math.*, **291**, 197 (2016); https://doi.org/10.1016/j.cam.2015.03.040.

32. T. LIU and Z. WU, "Adjoint Solution of Time-Dependent Multigroup Diffusion Model with Generalized Temporal and Spatial Boundary Conditions," *Proc. American Nuclear Society Student Conference*, Virtual Meeting, April 8–10, 2021.

33. L. HUANG, "Use of Adjoint Space Models for Predicting the Response of a Neutron Detector to Core Parametric Fluctuations," PhD Dissertation, Iowa State University (1979).

34. A. MISHRA et al., "Time Dependent Adjoint-Based Optimization for Coupled Fluid–Structure Problems," *J. Comput. Phys.*, **292**, 253 (2015); https://doi.org/10.1016/j.jcp.2015.03.010.

35. Y. CAO et al., "Adjoint Sensitivity Analysis for Differential-Algebraic Equations: The Adjoint DAE System and Its Numerical Solution," *SIAM J. Sci. Comput.*, **24**, *3*, 1076 (2003); https://doi.org/10.1137/S1064827501380630.